Nuclear Levels in ^{142}Pr†

JEAN KERN
Physics Department, University of Fribourg, Fribourg, Switzerland
and
The Florida State University, Tallahassee, Florida
AND
GORDON L. STRUBLE
Department of Chemistry, University of California, Berkeley, California
AND
RAYMOND K. SHELINE
The Florida State University, Tallahassee, Florida
AND
E. T. JURNEY
Los Alamos Scientific Laboratory, University of California, Los Alamos, New Mexico
AND
H. R. KOCH, B. P. K. MAIER, U. GRUBER, AND O. W. B. SCHULT
Physik-Department der Technischen Hochschule München, München, Germany
and
Research Establishment of the Danish Atomic Energy Commission, Risø, Denmark
(Received 22 March 1968)

A combination of (d,p)-reaction spectroscopy and high- and low-energy γ rays following thermal-neutron capture in ^{141}Pr has been used to study the levels in ^{142}Pr. The (d,p) reaction populates 65 states below 2 MeV, whereas 37 states below 2 MeV are populated by high-energy γ transitions from thermal-neutron capture. The ground-state Q value determined in the (d,p) reaction is 3622 ± 3 keV, in agreement with the neutron binding energy of 5843.4 ± 1.5 keV. Differential cross sections were measured at nine angles for the (d,p) reaction and interpreted in terms of the distorted-wave Born-approximation reaction theory. Utilizing, in addition, some of the low-energy γ rays observed with a bent-crystal spectrograph and with a Ge(Li) spectrometer, it has been possible to make the following assignments (energy in keV, spin and parity in parentheses): ground state, (2−); 3.683, (5−); 17.740, (3−); 63.746, (6−); 72.294, (4−); 84.998, (1−); 128.251, (5−); 144.587, (4−); 176.863, (3−); and 200.525, (2−). These states are interpreted in terms of configuration mixing between the two configurations $\pi d_{5/2}{}^{1}\nu f_{7/2}{}^{1}$ and $\pi g_{7/2}{}^{-1}\nu f_{7/2}{}^{1}$. Not only the energies of the levels but also the transition probability ratios are consistent with this interpretation. The calculated half-life of the 3.683 keV, 5− isomeric state is in reasonable agreement with the experimental value. Tentative spin and parity assignments have been made to levels above 250 keV.

I. INTRODUCTION

THE level structure of ^{142}Pr can only be studied by reaction spectroscopy because both the neighboring isobars ^{142}Nd and ^{142}Ce are stable. However, structure studies of ^{142}Pr by the (d,p) reaction have been done by Fulmer *et al.*,[1] and Bingham and Sampson,[2] and high-energy γ rays following thermal-neutron capture were measured by Bartholomew and Kinsey[3] with a magnetic pair spectrometer and by Hughes *et al.*[4] Low-energy γ rays from thermal-neutron capture[5] have also been previously measured. But all this work has not disclosed details of the structure in this nucleus. This demonstrates the importance of the combined experimental approach which we are presenting in this paper and the need for considerably better resolution in all the experiments. We have approached the problem by using three different nuclear reaction spectroscopic methods. The experiments are (a) proton spectroscopy utilizing magnetic analysis of the reaction ^{141}Pr$(d,p)^{142}$Pr, which was performed at Florida State University,[6] (b) high-

† Work supported under the United States and Danish Atomic Energy Commissions and Fonds National Suisse de la Recherche Scientifique. Research at the Florida State University Tandem Van de Graaff was supported by the U. S. Air Force Office of Scientific Research under Contract No. AFOSR-62-423 and by the Nuclear Program of the State of Florida.

[1] R. H. Fulmer, A. L. McCarthy, and B. L. Cohen, Phys. Rev. **128**, 1302 (1962).

[2] F. W. Bingham and M. B. Sampson, Phys. Rev. **128**, 1796 (1962).

[3] G. A. Bartholomew and B. B. Kinsey, Can. J. Phys. **31**, 1025 (1953).

[4] L. B. Hughes, T. J. Kennett, and W. V. Prestwich, Nucl. Phys. **89**, 241 (1966).

[5] M. Giannini, G. Pinto, D. Prosperi, and S. Sciuti, Nuovo Cimento **29**, 977 (1963); A. F. Para and M. M. Bettoni, Energ. Nucl. **11**, 612 (1964).

[6] J. Kern, G. L. Struble, and R. K. Sheline, Bull. Am. Phys. Soc. **10**, 512 (1965).

and low-energy γ-ray spectroscopy using a Ge detector and the reaction ^{141}Pr$(n,\gamma)^{142}$Pr with thermal neutrons at Los Alamos, and (c) low-energy neutron capture γ-ray spectroscopy using the curved crystal spectrometer at Risø.

If phonon coupling is not too great the structure of the lowest-energy states in ^{142}Pr should be characterized by the last odd proton and the last odd neutron. In both ^{141}Pr and ^{143}Pr the ground state has spin and parity $\frac{5}{2}+$. A very low-lying $\frac{7}{2}+$ state is observed at 145 keV in ^{141}Pr and at 57.4 keV in ^{143}Pr. Presumably the ground states correspond to the $(\pi d_{5/2}{}^1)$ configuration and, in the case of the excited states, to the $(\pi g_{7/2}{}^{-1})$ configuration. The 83rd neutron in all known cases has spin and parity $\frac{7}{2}-$, which in the shell model is characterized by the $(\nu f_{7/2}{}^1)$ configuration. In the simplest shell-model scheme for ^{142}Pr, then, one expects six states from the $(\pi d_{5/2}{}^1\nu f_{7/2}{}^1)$ configuration with spins from 1− to 6− and eight states from the configuration $(\pi g_{7/2}{}^{-1}\nu f_{7/2})$ with spins from 0− to 7−. These two sets of states should both lie very low in the spectrum. The spectroscopy is quite similar to that in ^{140}La.[7] Since the configuration of the target ^{141}Pr is $\pi d_{5/2}{}^1$ and since the two configurations in ^{142}Pr can be expected to mix considerably, twelve of these fourteen expected states should be observed in the reaction ^{141}Pr$(d,p)^{142}$Pr. In the reaction ^{141}Pr$(n,\gamma)^{142}$Pr, assuming that both compound states 2+ and 3+ are formed through thermal-neutron capture, eight states (two sets of states with spins 1− to 4−) can be populated through primary high-energy $E1$ transitions.

In Sec. II we briefly describe the experimental techniques and present the results. Section III is concerned with the detailed interpretation of the level scheme up to 250 keV and a qualitative discussion of the higher-energy states. In Sec. IV we summarize the conclusions of our work.

II. EXPERIMENTAL METHOD AND RESULTS

A. (d,p) Experiment

1. Experimental Method

The (d,p) experiments were performed in the Tandem Van de Graaff Laboratory of the Florida State University. The analysis of the data of ^{141}Pr follows the same procedure and method as that used for ^{140}La.[7]

Targets were prepared by evaporating Pr_6O_{11} [8] onto thin carbon backings using electron bombardment.[9] They were exposed to the 10-MeV deuteron beam of the Tandem Van de Graaff and the emerging protons were analyzed in a single-gap Browne-Buechner magnetic spectrograph.[10] An array of three 5×25-cm, 50-μ nuclear plates manufactured by Eastman Kodak served as a detector. Then the proton tracks were scanned in $\frac{1}{2}$-mm strips under microscopes equipped with calibration stages. A typical spectrum is shown in Fig. 1.

The intense ^{13}C and ^{17}O peaks were used for the calibration of the energy of the incident deuteron beam. The exact positions of these peaks are obtained by short exposures which were often made before and after the main experiment in order to test the stability of the magnet.

The spectra were analyzed by use of a nonlinear least-squares computer code[11] in order to determine the individual components of the spectrum. This method of analysis was necessary because many of the peaks are unresolved. The position of the peaks, as determined by the least-squares analysis, was then entered in another code written for an IBM 709 computer in order to extract Q values and excitation energies. This code also determined if any of the peaks were caused by an impurity.

Absolute cross sections were obtained with the help of additional Rutherford scattering experiments at 4 MeV performed prior to and/or after the (d,p) experiment.

2. Results

Nine exposures were taken at angles ranging from 15° to 105°. Table I summarizes some of the details of the experiment. The resolution given here is the full width at half-maximum (FWHM) of the peaks close to the ground state. It was found that the FWHM increases slowly along the plates progressing toward smaller proton energies. It is about 2–3 keV larger at 2-MeV excitation than the values given in Table I. Because of instabilities in the deuteron beam energy, the data taken at 90° are very poor and they have been only partially analyzed and used. The differential cross section corresponding to one track is given as a measure of the ultimate sensitivity.

As will be shown conclusively in Sec. III, the first peak, designated g.s. in Fig. 1, is actually a doublet

TABLE I. Summary of the (d,p) exposures.

Angle (deg)	Exposure (μC)	Resolution FWHM (keV)	Average cross section per track (μb/sr)	Ground-state Q Value (keV)
15	5100	14.5	0.42	3623.0
25	10000	12.6	0.19	3623.4
35	6010	11.0	0.65	3622.7
45	7500	13.0	0.46	3623.8
55	6000	13.9	0.36	3621.5
65	6000	11.5	0.41	3618.2
75	10210	11.9	0.24	3621.3
90	6600	23.0	0.25	3622.3
105	8000	13.7	0.31	3623.5

[7] J. Kern, G. L. Struble, and R. K. Sheline, Phys. Rev. **153**, 1331 (1967).

[8] Spectroscopically pure Pr_6O_{11} was provided by Johnson, Matthey and Co., London.

[9] M. C. Olesen and B. Elbek, Nucl. Phys. **15**, 26 (1960).

[10] C. P. Browne and W. W. Buechner, Rev. Sci. Instr. **27**, 899 (1956).

[11] R. H. Moore and R. K. Zeigler, Los Alamos Scientific Laboratory Report No. LA-2367 (unpublished).

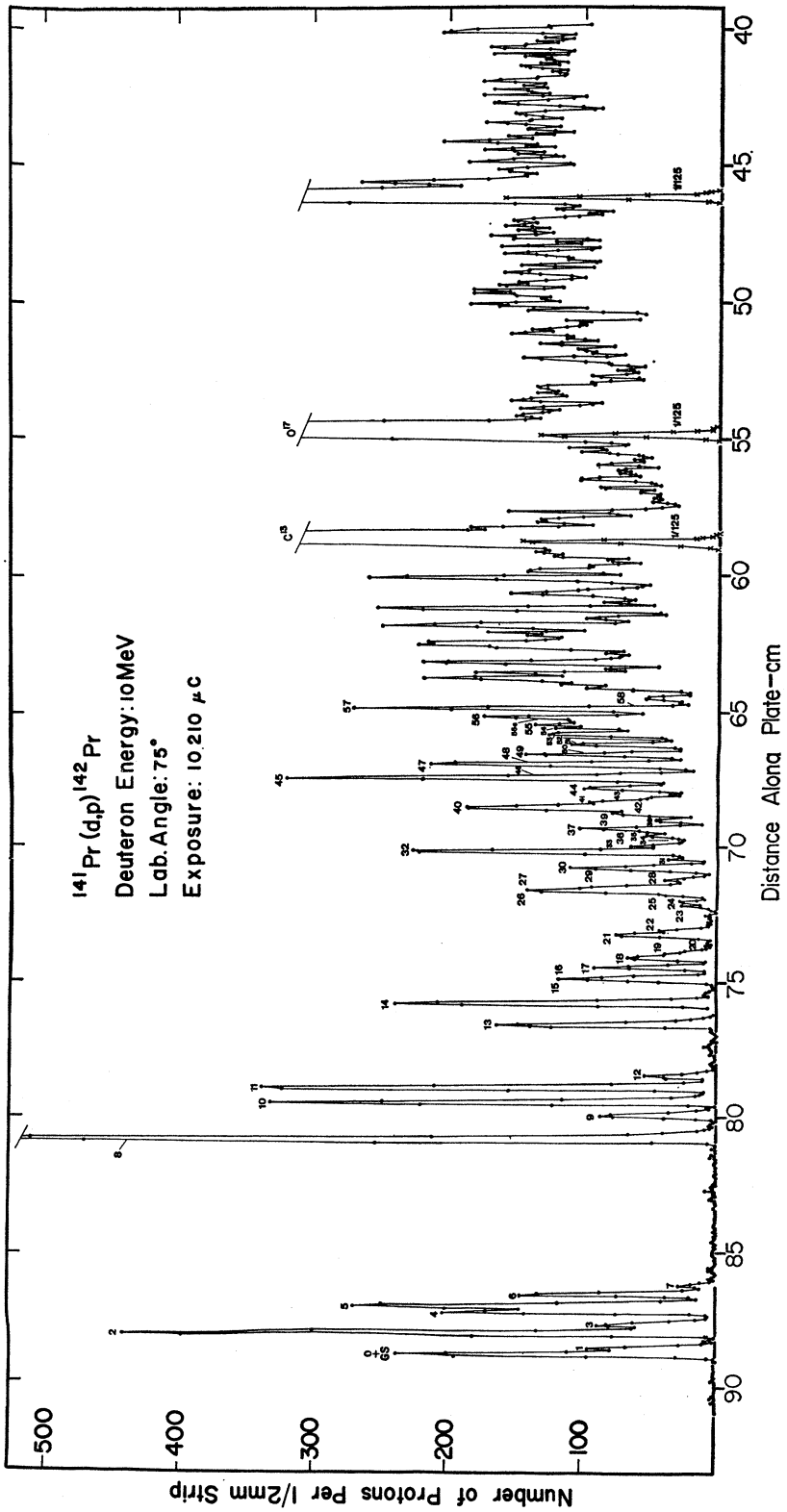

FIG. 1. Typical proton spectrum from the reaction ^{141}Pr$(d,p)^{142}$Pr.

whose two components are approximately equal in intensity. For this reason the observed Q values must be corrected by 1.6 keV. In Table II the values are corrected for the difference between the ground state and the combined peak centroid positions. The agreement between the values determined at different angles is very satisfactory. The average ground-state Q value is 3622.2 ± 0.6 keV. The fact that the Q value reproduces so well, even though the plate distance from the calibration (Carbon) peak to the ground-state peak varies considerably, indicates that the systematic errors are probably small. Therefore we give the value of $Q=3622\pm3$ *keV*. This value is compared with the results of other experiments in Sec. II C.

Table II gives the values of the level energies and differential cross sections. For the energies, standard deviations have been computed from the deviation of the single values from the average. For the intensities they are statistical sums of the standard deviation calculated from the fitting program, the error in the solid-angle calibration, and the error contributed by the Rutherford experiment, which is estimated to be 5%.

Nonstatistical errors may arise from an error in the energy calibration, use of an approximate fitting function (which may be important in the case of close multiplets), presence of impurities, an incorrect number of components in the analysis, or errors related to the process of scanning the plates.

With regard to energies, the error on the calibration was initially estimated to be about 0.5 keV up to 1-MeV excitation, and 1 to 2 keV above that excitation energy. Comparison with the excitation energies deduced from the (n,γ) experiments (see Table XV) suggests that this estimate is valid. The effect of this calibration error is expected to be smooth, so that the energy difference between levels not too distant is affected little by this error. Therefore the standard deviations have not been increased and must be considered as relative errors, i.e., errors which apply to the energy difference between relatively close levels. For a more detailed discussion of the problem of errors see Ref. 7.

In Table III we compare our results with those of Bingham and Sampson[2] and Fulmer *et al.*[1] Our cross sections are in fair agreement with the values of Bingham and Sampson, while the values of Fulmer *et al.* seem to disagree with our results by a factor of approximately two.

3. *Angular Distributions*

The angular distributions were fitted with the DWBA code TSALLY of Bassel, Drisko, and Satchler.[12] For the deuteron potential we extracted values from the work of Perey and Perey,[13] using set A without change. For the proton potential, we took values deduced from an article by Perey.[14] We found that a slight modification of the real radius from 1.25 to 1.21 was necessary. The parameters used are given in Table IV. Using these parameters and the "independent Saxon plus derivative" option with a lower cutoff radius of 5 F, we obtained the fits shown in Fig. 2.

The fits obtained are very satisfactory. It is possible that small adjustments of the optical potential parameters compensate for some of the experimental errors. The fact that our experimental distribution could be fitted so well is our only evidence that the reaction under study is essentially direct.

The use of the least-squares code to analyze the data has generally resulted in little dispersion in energy values for components of unresolved multiplets. The intensities, however, often have large uncertainties. For this reason it is better, in general, to compare only the intensity sum of badly resolved or unresolved peaks with theoretical curves. A meaningful result can be obtained only if the l transfer is the same for each of the components. The angular distributions of such groups are plotted in Fig. 2 together with the calculated curves.

B. High-Energy (n,γ) Spectrum

The target nucleus, monoisotopic ^{141}Pr, has a ground-state spin of $\frac{5}{2}^+$. Capture of s-wave neutrons can lead to compound states in ^{142}Pr with a spin and parity of 2^+, 3^+, which can decay by primary dipole transitions to states with spin 1, 2, 3, or 4. Electric dipole transitions will occur to states of negative parity, and generally weaker magnetic dipole transitions to states of positive parity. It is assumed that the high-energy part of the spectrum represents dipole transitions, which directly excite levels up to an excitation energy of ~2 MeV in ^{142}Pr.

The thermal-neutron capture cross section has been determined in several experiments. Activation experiments gave the result $\sigma_{act}=(10.9\pm1)$ b [15] and (10.8 ± 1) b.[16] On the other hand an absorption experiment gave the result $\sigma_{abs}=(11.3\pm0.2)$ b.[17] Since the only reaction which should effectively contribute to the absorption is the (n,γ) reaction, we have adopted the more precise latter value of Cummings.[17]

Both high-energy ($E>3.5$ MeV) and low-energy ($E<1.5$ MeV) portions of the γ-ray spectrum from ^{142}Pr$(n,\gamma)^{142}$Pr were studied with the Los Alamos internal target capture γ-ray facility. The spectrometer uses a Ge(Li) detector (3-mm depletion depth, 1-cm^3 volume) placed inside a large NaI annulus. At high energies the system is used as a double-escape pair spectrometer, and at low energies the NaI annulus is

[12] R. H. Bassel, R. M. Drisko, and G. R. Satchler, Oak Ridge National Laboratory Report No. ORNL-3240 (unpublished).
[13] C. M. Perey and F. G. Perey, Phys. Rev. **132**, 755 (1963).
[14] F. G. Perey, Phys. Rev. **131**, 745 (1963).
[15] W. S. Lyon, Nucl. Sci. Eng. 8, 378 (1960).
[16] Brookhaven National Laboratory Report No. BNL 325, Suppl. 1, 2nd ed., 1960 (unpublished).
[17] J. D. Cummings, Atomic Energy Research Establishment Report No. *R/R* 2333, quoted in Brookhaven National Laboratory Report No. BNL 325, Suppl. 1, 2nd ed., 1960 (unpublished).

TABLE II. Level energies (in keV) and differential cross sections (in μb/sr) for the reaction ^{141}Pr$(d,p)^{142}$Pr. The standard deviation is given beneath each value. For the levels where a background has been subtracted—tail of ^{13}C or of ^{17}O—and which are denoted by an asterisk, the error is estimated.

Level	Energy	Differential cross section 15°	25°	35°	45°	55°	65°	75°	105°	Comments
g.s.	0.0									
0	3.2	66	81	154	233	297	234	221	170	
	1.5	5	5	14	17	18	16	13	14	
1	17.8	13	25	45	103	63	84	76	46	
	0.6	2	3	7	11	6	9	6	8	
2	63.7	130	125	300	450	519	461	404	331	a
	0.2	8	8	20	28	29	27	22	20	
3	86.2	22	23	55	108	88	83	84	52	b
	0.7	2	2	5	10	7	8	6	5	
4	128.0	64	55	118	156	206	183	176	148	c
	0.4	6	4	11	13	15	14	11	12	
5	144.6	68	75	195	241	282	267	246	167	
	0.4	7	6	16	20	18	18	14	13	
6	176.8	51	42	103	134	160	147	127	109	d
	0.3	6	4	9	11	10	11	9	8	
7	200.8	30	12	29	29	31	30	21	14	e
	0.5	3	2	5	5	4	3	3	2	
8	637.2	358	373	456	526	621	583	567	289	f
	0.5	21	21	30	34	35	33	30	16	
8a	664.9	8	6	4	72	7	14	2	3	g,h
	1.5	3	1	3	9	2	3	1	1	
8b	681.6	6	5	10	16	2	3	4	2	h
	0.7	2	1	3	4	1	1	1	1	
9	705.8	43	52	73	81	91	81	72	36	
	0.4	5	4	8	10	7	6	14	3	
10	748.2	168	188	261	287	318	253	264	139	
	0.6	11	12	20	21	20	16	17	9	
10a	767.0	4	6	10	19	31	11	10		h,i
	0.8	2	2	5	4	6	3	2		
11	792.1	188	198	276	297	322	298	287	153	j
	0.6	12	12	19	21	20	19	18	9	
12	823.5	32	28	23	56	35	38	41	21	
	0.7	5	2	4	6	4	4	4	4	
13	981.3	95*	88	134	136	156	143	128	75	k
	0.7	30	6	20	10	11	9	8	6	
14	1045.2		144	210	219	239	197	202	108	l
	0.7		10	15	14	16	12	13	7	
15	1115.4		70*	58	(28)	94	52	50	10	m,n
	1.2			8		13	14	13	3	
16	1127.2		11*		(50)	43	58	68	55	m
	1.8					11	14	13	5	
17	1154.4	59*		68	77	83	78	72	34	
	0.9	20		13	6	7	8	6	3	
18	1183.3	36*		240	56	51	41	59	38	o
	1.1			16	5	7	5	5	5	
19	1200.4	17*		44	34	43	48	28	19	
	1.1			5	4	7	8	3	6	
20	1220.2	19*		14	7	6	9	6	8	
	1.7			2	2	1	2	2	6	
20a	1236.6			9	7		4	5	5	h
	1.0			2	2		2	2	1	
21	1255.2	41*		64	74	65	54	63	31	
	0.7	20		6	6	7	5	5	3	
22	1269.6	28*		33	148	37	44	30	21	p
	1.4	10		6	12	4	5	3	3	
23	1348.2	28*	12*		17	14	15	11	19	q
	1.1				3	3	4	3	3	
24	1362.7	9*	9*		10	18	12	19	15	r
	1.7				2	3	3	3	2	
25	1381.5	24*	9*		16	21	16	25		
	1.4	10	5		4	15	4	7		
26	1395.2	46*	55*		96	167	117	106	55	s
	1.0	15	10		12	15	11	14	7	
27	1408.2	50*	38*		71	85	58	51	74	t
	0.6	15	10		11	13	8	5	7	
28	1428.9	23*	27*		38	30	33	27	24	u
	1.0	10	10		5	3	5	5	3	
28a	1444.7	24*	24*		8		8	7	11	h,v
	1.5	10	10		3		2	5	2	
29	1462.7	66*	47*	94*	46	20	62	42	66	w
	1.3	30	10	20	5	9	9	4	11	
30	1473.5	63*	13*	26*	52	87	38	63	14	x
	1.5	30	5	12	11	11	8	10	10	
31	1499.1	25*	43*	31*	33	26	18	24	17	y
	1.0	10	8	15	5	3	3	3	3	

TABLE II (*Continued*).

Level	Energy	Differential cross section 15°	25°	35°	45°	55°	65°	75°	105°	Comments
32	1519.8	81*	107*	189*	178	213	253	189	126	z
	0.6	15	10	25	15	14	17	13	9	
33	1540.1	13*	24*	51*	39	30	43	44	38	aa
	0.6	5	5	15	8	3	5	5	4	
34	1556.0	16*	30*	17*	30	19	21	18		ab
	1.3	5	5	10	7	7	4	4		
35	1570.7	19*	19*	65*		42	42	37	26	ac
	1.2	5	5	7		4	5	6	3	
36	1586.7	27*	34*	72*		19	65	26	30	ad
	1.4	8	8	10		7	12	9	4	
37	1597.4	13*	14*	28*		76	21	68	72	ae,af
	1.2	7	5	6		10	12	13	6	
38	1621.6	22*	13*	59*		34	34	40	27	aa
	0.4	10	10	10		4	4	4	3	
39	1642.6	32*	37*	71*		56	64	61	37	ag
	0.6	10	8	10		6	6	6	4	
40	1660.1	44*	59*	90*		121	111	163	56	ah
	0.6	10	8	16		10	9	12	5	
41	1677.2	28*	43*	87	62*	79	94	81	57	ai
	0.8	20	8	10		8	8	7	6	
42	1693.5	23*	25	38	54*	36	38	41	28	
	1.8	15	5	7		5	4	5	4	
43	1711.2	23*	25*	30	43*	22		34	28	
	1.9	10	5	8	15	15		8	4	
44	1725.8	45*	43	82	41*	95	60	72	58	aj
	0.9	15	5	12	20	19	12	9	6	
45	1755.2	101*	124	196	230*	277	249	241	162	
	0.6	15	10	16	20	19	17	17	15	
46	1771.5	27*	30	53	63	49	33	51	37	
	0.5	15	5	8	8	17	5	5	9	
47	1799.5		73	132	144	189	169	161	94	
	0.9		8	12	17	12	17	12	16	
48	1811.9		38	26	53		29	15	27	
	1.3		6	6	14		8	5	14	
49	1832.3		50*	83	92	114	107	99	69	
	0.9		8	10	7	12	10	10	7	
50	1845.1		44*	37	48	38	24	26	13	ak
	0.8		10	13	9	9	6	8	6	
51	1866.2		51*	65	101	131	76	89	58	
	0.8		5	7	9	10	7	8	6	
52	1884.6			19	21		14	27	14	
	0.9			4	6		3	5	4	
53	1900.8			112	92		121	107	73	
	0.6			11	10		13	10	8	
54	1919.4			65	66		83	68	61	
	0.5			9	9		11	17	5	
55	1934.9	61*		59	104		97	80	65	
	0.9			9	10		12	14	5	
55a	1947.3			94				60	45	h
	0.9			16				14	5	
56	1957.4	43*		46	144		145	123	64	
	1.1			16	13		11	17	5	
57	1982.9	135*			177		169	190	110	
	0.9				14		14	14	9	
58	2001.2	82*			31		20	15	12	
	2.5				6		6	5	5	
59	2015.5	12*			53				40	
	2.4				7				6	

At 90° the differential cross section for the group of peaks g.s. to 7 is 1236±88 μb/sr; it is 874±67 μb/sr for the peaks 8+9+10+11. In the following the estimated contributions of the impurities are given between parentheses (μb/sr); they should be subtracted from the measured cross sections. The notation indicates the level number in the final nucleus; for instance 5^{183}W refers to the fifth level (from ground) populated in the reaction ^{182}W$(d,p)^{183}$W.

[a] 5^{183}W at 15° (10).
[b] 3^{29}Si at 45° (25).
[c] 7^{32}P at 15° (5).
[d] 5^{33}S at 15° (10).
[e] 11^{36}Cl at 15° (15), ^{29}Si at 55°.
[f] Cross section at 90° is 380±24 μb/sr.
[g] 7^{33}S at 45° (60).
[h] Doubtful level. The differential cross section undergoes erratic changes and the energy does not reproduce very well at all angles.
[i] 7^{32}S at 55° (20).
[j] 4^{24}Na at 15° (10).
[k] 4^{29}Si at 65°; cross section at 90° is 101±8 μb/sr.
[l] Cross section at 90° is 162±12 μb/sr.
[m] The plate edges fall on peaks 16 at 35° and on peaks 15 and 16 at 45°. The corresponding cross sections are therefore rather uncertain.
[n] 4^{29}Si at 75°.
[o] 5^{29}Si at 35° (200).
[p] 5^{29}Si at 45° (120).
[q] 11^{33}S at 15° (20).
[r] 7^{33}S at 105°.
[s] 11^{33}S at 25° (15); 5^{29}Si at 55° (80).
[t] 12^{33}S+4^{38}Cl at 15° (20).
[u] 6^{24}Na at 15°.
[v] 5^{38}Cl at 15°, 12^{33}S+4^{38}Cl at 25° (15).
[w] 11^{33}S at 35° (30).
[x] 6^{38}Cl at 15° (50).
[y] 6^{38}Cl at 25°, 4^{38}Cl at 35° (10).
[z] 12^{33}S at 35° (20), 5^{29}Si at 65° (40).
[kk] The energy value is a corrected average.
[ab] 6^{29}Si+7^{38}Cl at 25°.
[ac] 8^{38}Cl at 15° (10), 6^{38}Cl at 35° (30).
[ad] 7^{24}Na at 25° (5); 6^{24}Na at 35° (30).
[ae] 8^{38}Cl at 25° (5).
[af] The energy value is a weighted average.
[ag] 6^{29}Si at 35° (10).
[ah] 5^{29}Si at 75° (60).
[ai] 7^{24}Na at 35° (20).
[aj] 9^{20}F at 35°.
[ak] 9^{38}Cl at 35° (10).

operated in anticoincidence with the Ge(Li) detector to reduce the background from escape events. In our experiments, the detector resolution (FWHM) varied from 3.6 keV at 300 keV to 7.5 keV at 5000 keV. Details of the arrangement have been described elsewhere.[18]

The target was prepared by pressing and sintering 2.1 gm of Pr_6O_{11} into a 23-mm-diameter disk, which was placed in a small graphite holder for insertion into the thermal column channel. The target material contained < 10-ppm contamination from rare-earth impurities.

The energy scale for the high-energy part of the spectrum is based on the values of Greenwood[19] for the $^{14}N(n,\gamma)^{15}N$ γ-ray energies. The efficiency of the spectrometer was calibrated with the transitions of the $^{14}N(n,\gamma)^{15}N$ spectrum, whose intensities are well known.[20,21] Using the thermal-neutron cross section (given above) of ^{141}Pr, we obtained absolute transition intensities expressed as number of photons per 10^3 captured neutrons.

Table V gives the energies and intensities of the observed transitions; Fig. 3 shows the double-escape spectrum with the peaks labeled according to the transition numbers in Table V.

The γ-ray energies in Table V do not show good overall agreement with the values reported by Hughes, Kennett, and Prestwich,[4] although the agreement is satisfactory for the ground-state transition. These authors do not observe the transitions at 5698.7 and 5641.1 keV (see Table V). However, they do report transitions of comparable intensity at 5598, 5452, 5390, and 5302 keV (two of which they indicate may be spurious peaks) which we did not observe.

C. Neutron Binding Energy of ^{142}Pr

The Q value as obtained in the (d,p) experiments is $Q=(3622\pm3)$ keV. (See Sec. II A 1 and 2.) Bingham and Sampson[2] give the value $Q=3540$ keV; the difference must be because of the difficulty in resolving the group of peaks containing the ground state. The MIT group[22] has obtained $Q=(3626\pm10)$ keV, which is in good agreement with our result.

From the Q value we deduce the binding energy for the last neutron to be (5847 ± 3) keV (using 2224.6 keV for the deuteron binding energy[23]). The energy of the highest-energy γ ray in the (n,γ) spectrum, assumed to represent a transition directly to the ground state of ^{142}Pr, is (5843.4 ± 1.5) keV. This value is in agreement with the value B_n determined in the (d,p) experiments and also with the (n,γ) value (5842 ± 5) keV reported by Hughes *et al.*[4]

TABLE III. Comparison of the absolute differential cross sections as determined in this work with the results of previous investigations. The values apply to the maximum cross sections in the (d,p) angular distributions.

Group of peaks	This work	$(d\sigma/d\Omega)_{max}$ in μb/sr Bingham[a]	Fulmer[b]
g.s. to 7	1650	1750	3120
8(636 keV)	620	1200	1350
10+11+12	675		1540
Estimated error	5%	30%	30%

[a] Reference 2.
[b] Reference 1.

TABLE IV. Optical-model parameters.

	"d" Potential	"p" Potential
Depth of real potential V_S (MeV)	74	55
Nuclear and charge radius r_{0S}, R_C (F)	1.15	1.21
Diffuseness of real potential a_S (F)	0.87	0.65
Depth of surface part of imaginary pot. W_D (MeV)	12	13.5
Radius of imaginary pot. r_{0I} (F)	1.37	1.25
Diffuseness of imaginary pot. a_I (F)	0.7	0.47

D. Low-Energy (n,γ) Spectrum

1. *Los Alamos Ge(Li) Spectrometer Results*

The experimental facility has been described in the preceding section. Table VI gives the energies and intensities of the γ rays up to ~1500 keV. A part of the spectrum is shown in Fig. 4.

Energies were determined through a calibration with well-known radioactive standards. The intensities in units of photons per 10^3 neutrons captured were determined by normalizing a previously determined curve of the detector sensitivity versus energy with the help of the intensity of the 411-keV ^{198}Hg line from a weighed gold foil. For this measurement, the gold standard was irradiated and counted while in the normal target position.

Target self-absorption corrections became severe at the lower energies. For this reason, and because of small variations in the target thickness, errors have not been quoted for the five lowest-energy lines in Table VI.

2. *Risø Curved-Crystal-Spectrometer Results*

The curved-crystal spectrometer[24] at Risø was also used for the measurement of the low-energy γ spectrum emitted during the irradiation of ^{141}Pr (and possible impurities) with slow neutrons. The source consisted of 43 mg of praseodymium oxide. The width δE

[18] E. T. Jurney, H. T. Motz, and S. H. Vegors, Jr., Nucl. Phys. A94, 351 (1967).
[19] R. C. Greenwood, Argonne National Laboratory Report No. ANL-7282 (unpublished).
[20] E. T. Jurney and H. T. Motz, Argonne National Laboratory Report No. ANL-6797, p. 236, 1963 (unpublished).
[21] H. T. Motz *et al.*, *Pile Neutron Research in Physics* (International Atomic Energy Agency, Vienna, 1962), p. 225.
[22] A Sperduto and W. W. Buechner, in *Proceedings of the Second International Conference on Nuclidic Masses, Vienna, 1963*, edited by W. H. Johnson (Springer-Verlag, Berlin, 1964), p. 289 ff.
[23] R. C. Greenwood and W. W. Black, Phys. Letters 21, 702 (1966).
[24] U. Gruber, B. P. Maier, and O. W. B. Schult, Kerntechnik 5, 17 (1963); B. P. Maier, U. Gruber, and O. W. B. Schult, *ibid.* 5, 19 (1963).

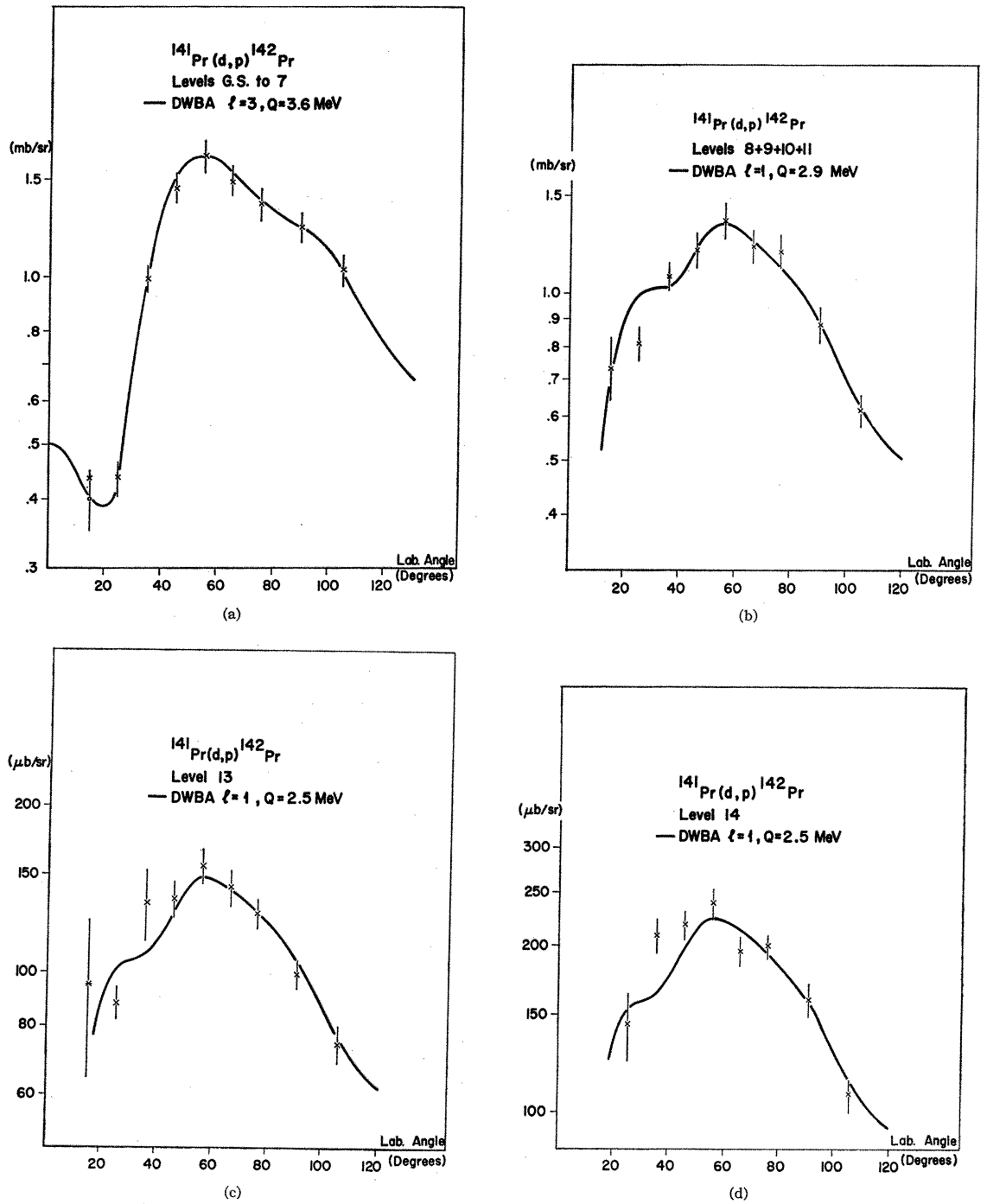

FIG. 2. Angular distributions of several different proton groups from the reaction ^{141}Pr$(d,p)^{142}$Pr. Experimental data are represented by crosses (×) or by asterisks (*) when a background was subtracted, or by a zero (0) when an impurity component was subtracted. A zero superposed on a cross indicates that both subtractions have been performed. (a) Levels at 0, (4), 18, 64, 86, 128, 145, 177, and 201 keV. (b) Levels at 637, 706, 748, and 792 keV. (c) Level at 981 keV. (d) Level at 1045 keV. (e) Level at 1154 keV. (f) Levels at 1255 and 1270 keV. (g) Levels at 1395 and 1408 keV. (h) Levels at 1463 and 1474 keV. (i) Levels at 1499, 1520, and 1540 keV. (j) Levels at 1571, 1587, and 1597 keV. (k) Levels at 1643, 1660, 1677, and 1694 keV. (l) Levels at 1755 and 1772 keV. (m) Levels at 1800 and 1812 keV. (n) Levels at 1832 and 1845 keV. (o) Levels at 1866, 1885, and 1901 keV. (p) Levels at 1919, 1935, (1947), and 1957 keV.

(Fig. 2 continued on next 3 pages)

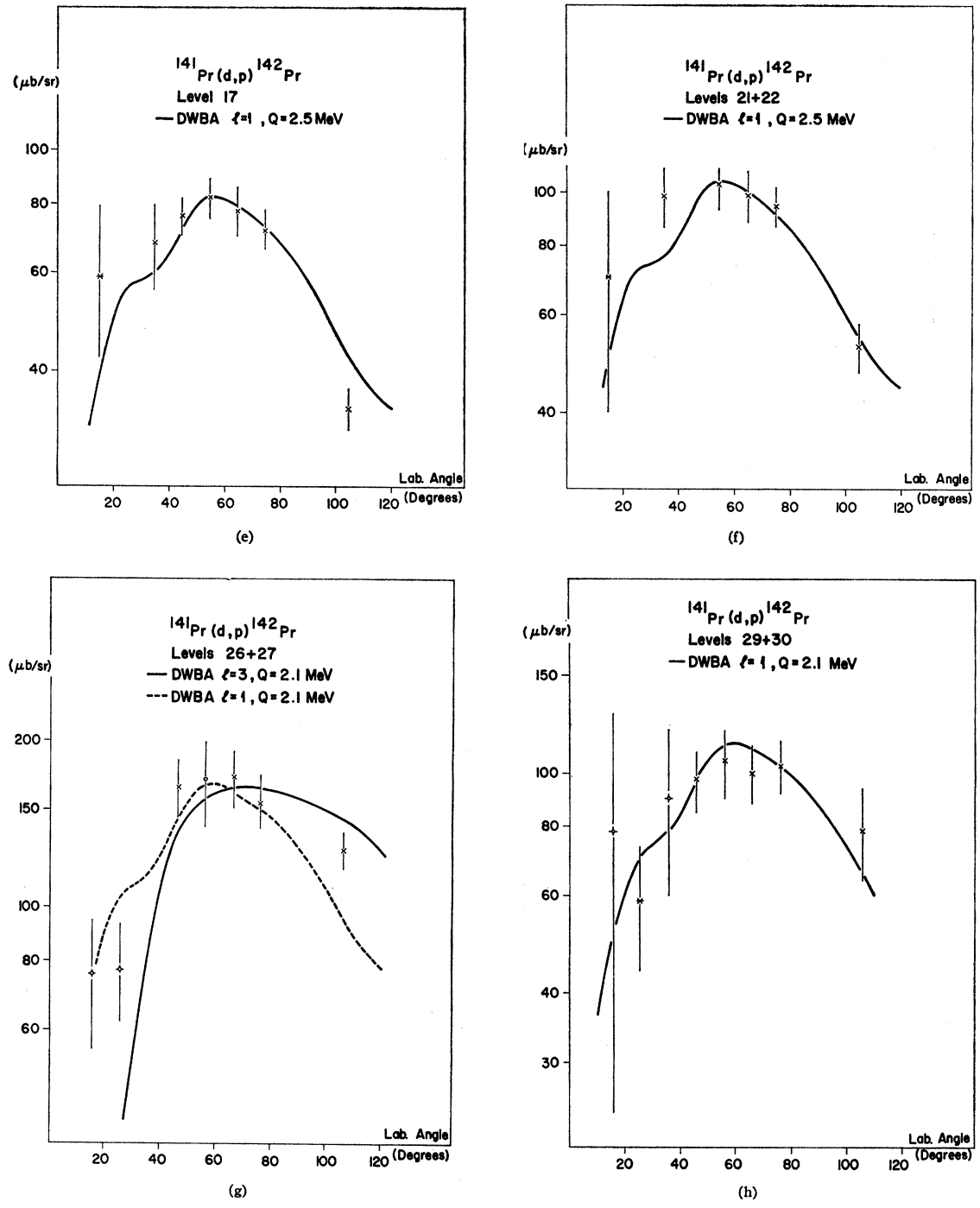

FIG. 2—*Continued.*

(FWHM) of the observed γ lines is

$$\delta E \approx 1.4\times10^{-5}\times E^2/n,$$

where E is the γ energy in keV and n is the order of reflection. Strong transitions were measured in the fifth-order reflection, weaker lines were studied in the third- or second- and occasionally in the first-order reflections.

The spectrum was scanned in the energy region from 26.5 keV up to about 1 MeV. Parts of the γ spectrum are shown in Fig. 5. Absolute γ energies were obtained using for calibration the K_α-x-ray energies of Pr and

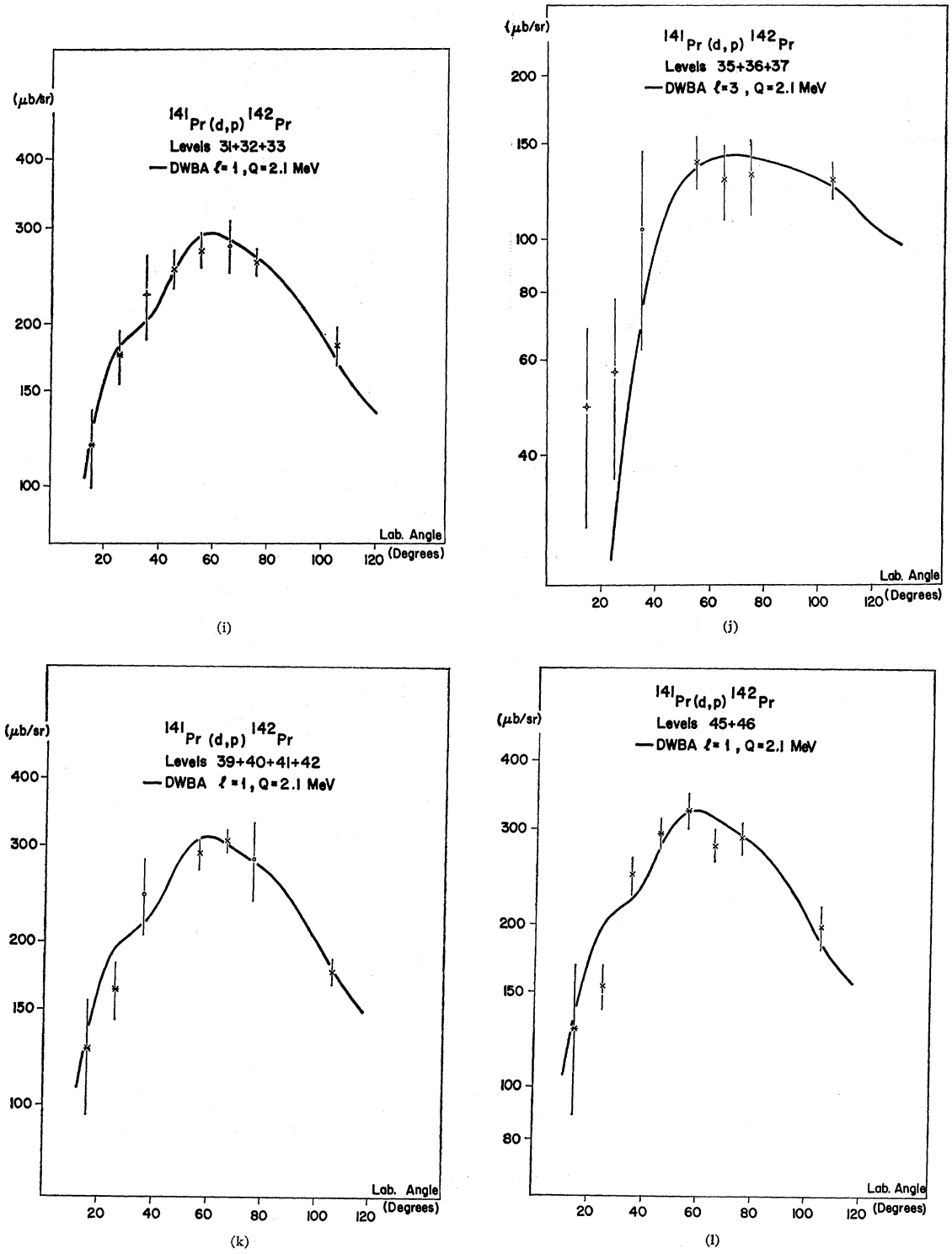

FIG. 2—*Continued.*

Er which have been measured very accurately by Bergvall.[25] Details of the measuring procedure and the evaluation of the data have been given elsewhere.[26] The results are listed in Table VI. Only relative γ

[25] P. Bergvall, Arkiv Fysik **16**, 57 (1960).

[26] O. W. B. Schult, U. Gruber, B. P. Maier, and F. W. Stanek, Z. Physik **180**, 298 (1964).

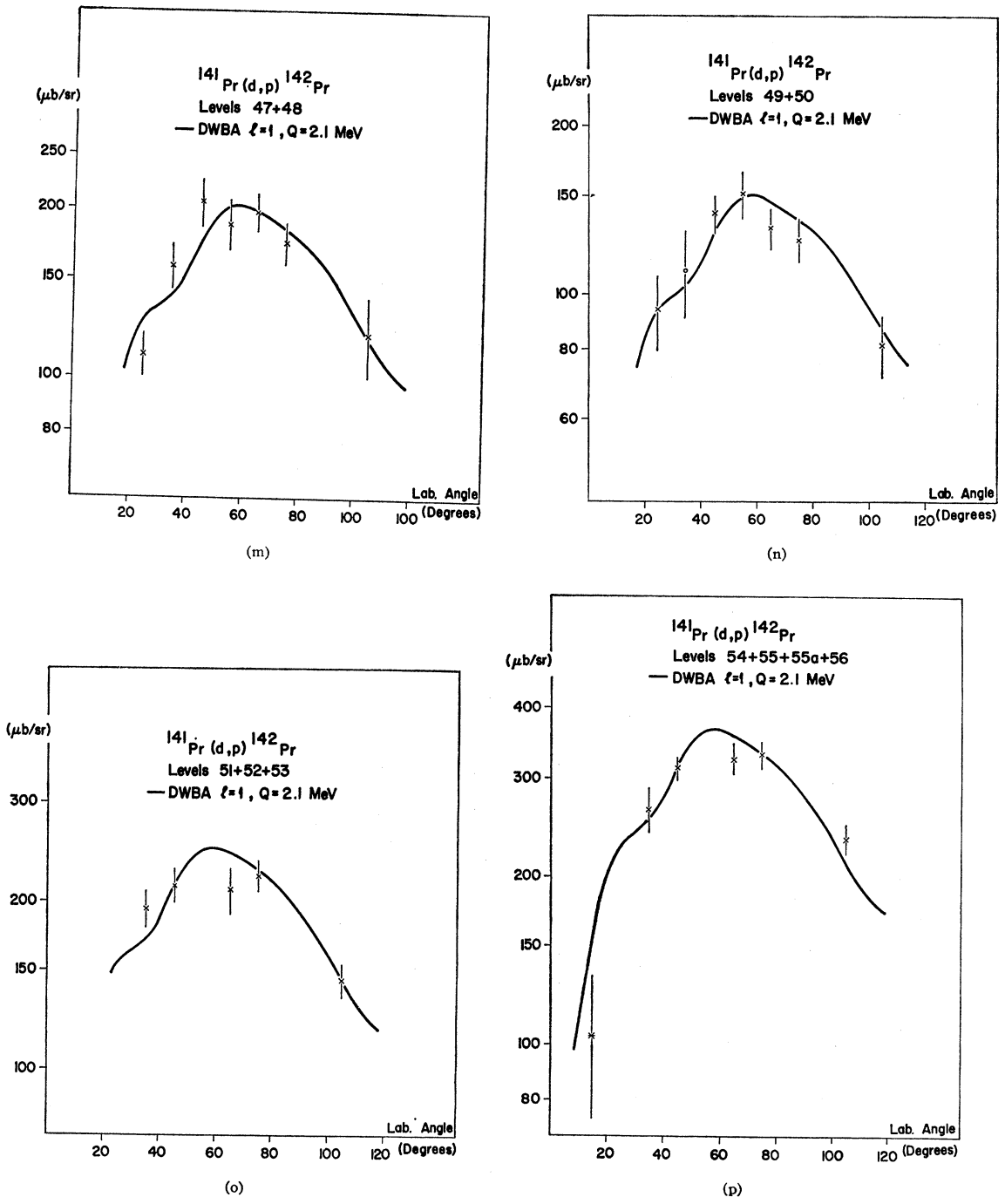

FIG. 2—*Continued.*

intensities were determined. The scale has been adjusted so that the numerical values correspond to the absolute intensities obtained in the Los Alamos experiment. The intensity errors as given in column 6 of Table VI include only the statistical uncertainty of the reflexes and part of the absorption correction error. Because of the poorly defined source geometry, the self-absorption within the source could be estimated only crudely, so that it may be necessary to apply an additional correction factor up to 1.3 when intensities of transitions of higher energy (>200 keV) are compared with those of lower energy (<100 keV). A comparison of these data with the results obtained with the Los Alamos Ge spectrometer indicates that several transitions seen in the curved-crystal spectrum are probably impurity lines. Unassigned impurity lines have been kept in the table;

TABLE V. $^{141}Pr(n,\gamma)^{142}Pr$. High-energy spectrum.

Transition number	E_γ (keV)[a]	E_{exc} (keV)[a]	dE_{exc} (keV)	I_γ ($\gamma/10^2 n$)[b]	dI_γ ($\gamma/10^2 n$)
1	5843.4	g.s.	...	15	3
2	5825.7	17.7	0.4	5.0	1.2
3	5771.5	71.9	0.5	3.4	0.8
4	5698.7	144.7	1.5	1.2	0.4
5	5666.4	177.0	0.2	42	9
6	5641.1	202.3	1.5	1.3	0.4
7	5206.3	637.1	0.3	4.0	0.9
8	5140.4	703.0	0.3	38	8
9	5096.2	747.2	0.3	21	5
10	5053.0	790.4	0.4	3.7	0.8
11	5020.4	823.0	0.6	1.7	0.5
12	4945.2	$^{12}C(n,\gamma)$	...	...	...
13	4864.6	978.8	1.5	1.5	0.4
14	4801.2	1042.6	0.3	16	3
15	4723.2	1120.2	0.3	11	2
16	4692.2	1151.2	0.3	32	7
17	4591.6	1251.8	0.7	1.6	0.5
18	4579.1	1264.2	1.2	0.9	0.4
19	4494.8	1348.6	0.3	11	2
20	4447.0	1396.4	0.8	1.8	0.5
21	4438.2	1405.2	0.6	3.1	0.7
22	4369.8	1473.6	0.5	3.3	0.9
23	4343.3	1500.1	1.2	1.5	0.4
24	4274.0	1569.4	0.4	5	1
25	4249.1	1594.3	0.5	4.3	0.9
26	4173.3	1670.1	0.7	3.8	0.9
27	4160.4	1683.0	0.8	3.0	0.8
28	4130.4	1713.0	0.8	3.3	0.8
29	4113.4	1730.0	2.2	1.1	0.4
30	4088.5	1754.9	0.5	2.1	0.6
31	4049.1	1794.3	1.5	1.2	0.4
32	4009.7	1833.7	0.6	2.5	0.6
33	3997.8	1845.6	0.9	1.5	0.4
34	3941.5	1901.9	1.0	2.7	0.7
35	3920.5	1922.9	0.8	3.3	1.1
36	3907.7	1935.7	0.7	4.5	0.9
37	3889.1	1954.3	0.6	4.0	1.3
38	3859.4	1984.0	1.0	1.6	0.5
39	3808.6	2034.8	1.0	2.2	1.0
40	3788.6	2054.8	0.4	16	3
41	3771.9	2071.5	0.8	3.2	0.8
42	3712.5	2130.9	0.5	4.6	1.0
43	3685	$^{12}C(n,\gamma)$	...	...	...
44	2678.9	2164.5	1.0	3.1	0.8
45	3661.2	2182.2	1.3	1.8	0.5
46	3652.9	2190.5	0.6	8.5	2
47	3647.0	2196.4	0.8	4.2	1.1
48	3603.0	2240.4	0.7	7	2
49	3584.5	2258.9	0.9	2.8	0.8
50	3563.8	2279.6	1.5	2.1	0.7
51	3553.1	2290.3	1.0	3.5	0.9
52	3537.5	2305.9	1.0	6	2

[a] Not corrected for nuclear recoil.
[b] Based on $\sigma_\theta = (11.3 \pm 0.2)$ b for ^{141}Pr (J. D. Cummings, Ref. 17).

if they can be identified as coming from some particular isotope, it will be possible to subtract the entire spectrum due to that impurity.

We have presented Ge(Li) and curved-crystal spectrometry results together in Table VI, in order to compare easily the two sets of data. At low energy the better resolution of the Risø facility discloses more details. The methods used at Risø and at Los Alamos are comparable at around 700 keV, and above this region the Ge diode gives better results.

In column 11 we have given transition assignments, which will be discussed in further sections. A considerable (~70%) percentage of the observed transitions has been accommodated in the level schemes (see Figs. 6 and 12).

III. INTERPRETATION OF RESULTS

A. Construction of the Level Scheme up to 250 keV

The similarity between ^{140}La and ^{142}Pr has been pointed out in the Introduction. We expect that the method of analysis which was successfully used[7] with ^{140}La is also valid when applied to ^{142}Pr.

^{142}Pr has 59 protons and 83 neutrons, corresponding to 9 protons and 1 neutron outside the doubly magic ^{132}Sn. In all our arguments we will assume that this core of 132 nucleons is inert to excitations and contributes only to a Hartree-Fock-like single-particle potential experienced by the 10 valence nucleons. The 83rd neutron may confidently be assigned to the $2f_{7/2}$ shell-model orbital from level systematics in neighboring odd-A nuclei. We may incorporate the important pairing correlations present in the proton system by using a quasiparticle description. In this picture, ^{142}Pr is a system with one shell-model neutron and one quasiproton. Again using level systematics of neighboring odd-A nuclei, we find that the lowest single quasiproton states are in the $2d_{5/2}$ and $1g_{7/2}$ orbitals. Other quasiparticle excitations are at sufficiently high energies that they can be neglected.[27] But we have also neglected the long-range correlations in the proton system due to interactions among the quasiparticles. For simplicity, we will consider these as harmonic quadrupole phonons. The neutron-proton interaction will cause configuration mixing between basis states $|j_p^0 j_n J; pR; IM\rangle$, where the quasiproton in the j_p^0 and the neutron in the state j_n couple to angular momentum J. Similarly p phonons couple to angular momentum R. The total angular momentum of the system is given by I. Using arguments presented in previous investigations,[27] we feel justified in attempting to describe the lowest excited states in the highly restricted two-dimensional space spanned by the vectors

$$|\pi 2d_{5/2}{}^0 \nu 2f_{7/2} J; 00; JM\rangle,$$
$$|\pi 1g_{7/2}{}^0 \nu 2f_{7/2} J; 00; JM\rangle.$$

Shortening the notation, we consider that for a given spin and negative parity we may write the states as

$$|JM\rangle_{1J} = \alpha_{1J}|\pi 2d_{5/2}\nu 2f_{7/2}; JM\rangle + \beta_{1J}|\pi 1g_{7/2}\nu 2f_{7/2}; JM\rangle,$$
$$|JM\rangle_{2J} = \alpha_{2J}|\pi 2d_{5/2}\nu 2f_{7/2}; JM\rangle + \beta_{2J}|\pi 1g_{7/2}\nu 2f_{7/2}; JM\rangle.$$

If we choose the phases so that the α's are positive, a necessary condition for the orthonormality of the state vectors is

$$|\beta_{1J}| = (1-\alpha_{1J}{}^2)^{1/2} = \alpha_{2J},$$
$$|\beta_{2J}| = \alpha_{1J}.$$

[27] G. L. Struble, Phys. Rev. 153, 1347 (1966).

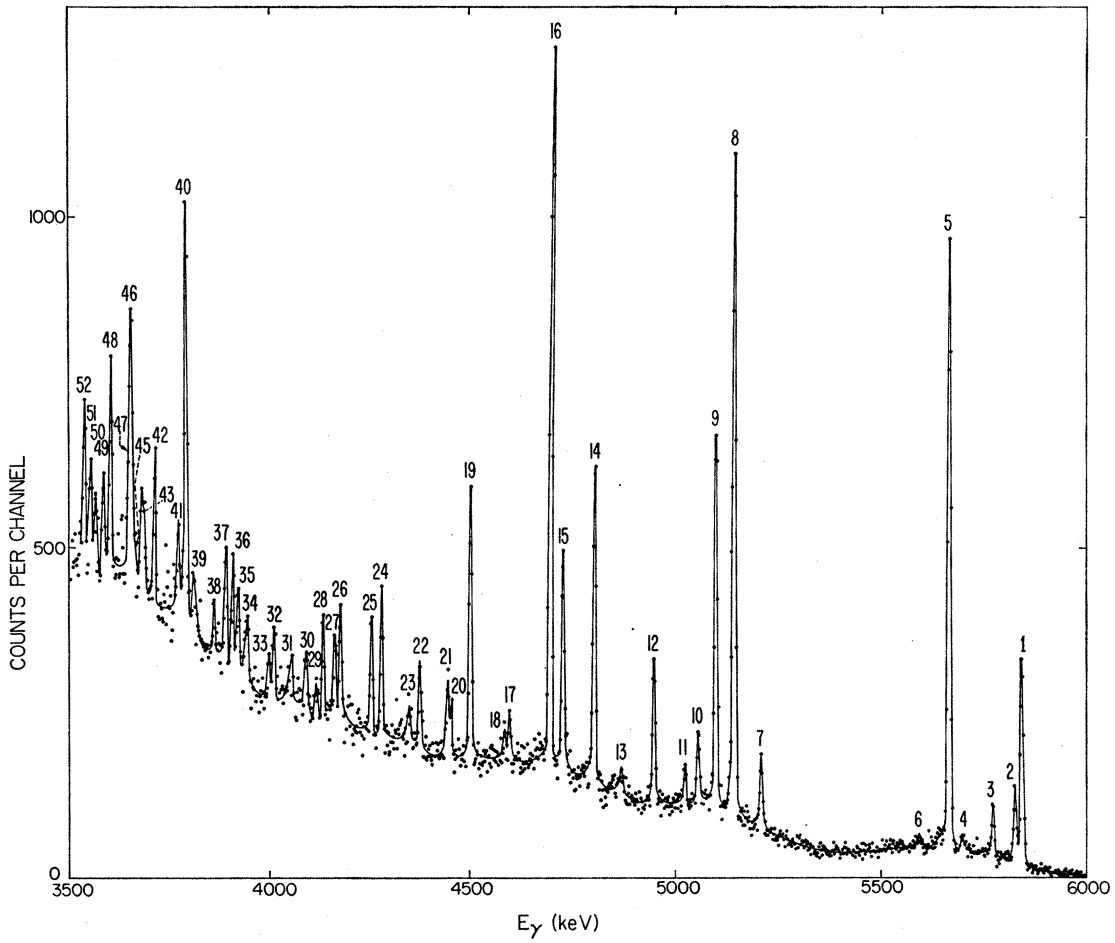

FIG. 3. Double escape peak (n,γ) spectrum of ^{142}Pr measured at Los Alamos. The numbering of the peaks is according to the transition numbers in Table V.

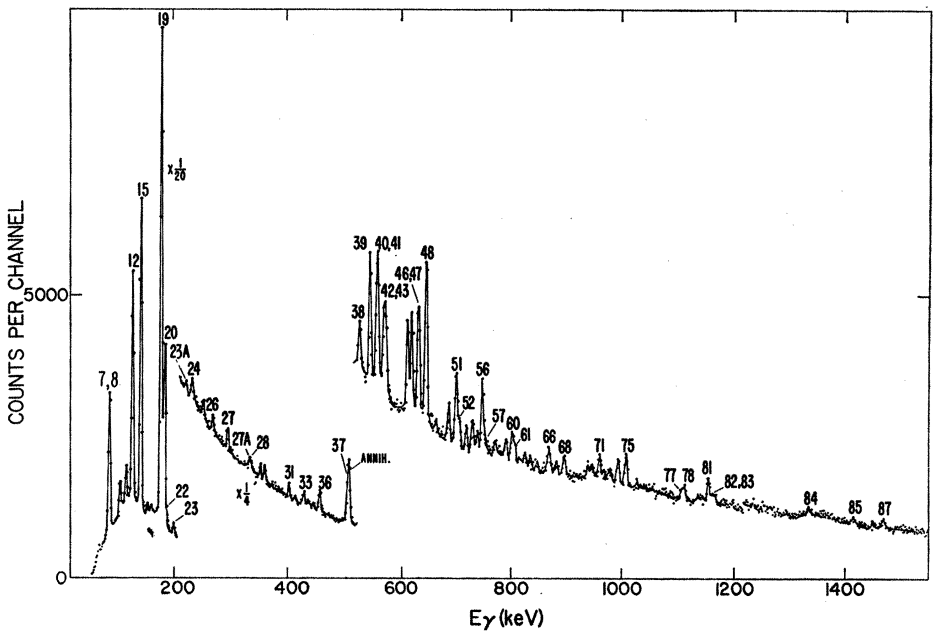

FIG. 4. A portion of the low-energy (n,γ) spectrum of ^{142}Pr measured with the Los Alamos Ge(Li) detector inside a NaI annulus in anticoincidence. The peaks are labeled according to the transition numbers of Table VI.

TABLE VI. $^{141}Pr(n,\gamma)^{142}Pr$. Low-energy transitions obtained with the diffraction and Ge(Li) spectrometers. In column 11 the "assignments" are given as the initial and final levels (denoted by their energies in keV) between which the transitions have been placed.

1	2	3	4	5	6	7	8	9	10	11	12
	Crystal spectrometer					Ge(Li) diode					
Trans. No.	E_γ (keV)	ΔE_γ (keV)	FWHM (keV)	I_γ (rel)	100. $\Delta I_\gamma/I_\gamma$	E_γ (keV)	ΔE_γ (keV)	I_γ ($\gamma/10^3 n$)[a]	ΔI_γ ($\gamma/10^3 n$)	Assignments E_i-E_f	Comments
1	32.278	0.006	0.015	2	···	32.5	2.5	5	···	176.9−144.6	
1a	···	···	···	···	···	47.3	0.6	3	···		
2	54.568	0.008	0.04	5.3	20	54.5	0.6	2	···	72.3− 17.7	
3	55.950	0.007	0.04	1.3	···	···	···	···	···	128.3− 72.3	
4	60.064	0.002	0.025	9.9	10	60.3	0.6	8	···	63.7− 3.7	
5	64.506	0.002	0.03	8.8	10	64.7	0.5	8	···	128.3− 63.7	
6	68.610	0.002	0.03	8.1	10	68.7	0.5	9	5	72.3− 3.7	
7	84.998	0.003	0.05	13	10	85.6	0.5	24	5	85.0− 0	
8	86.056	0.003	0.05	8.9	10						
9	104.569	0.004	0.08	3.5	10	105.3	0.6	3.5	1.4	176.9− 72.3	
10	115.529	0.005	0.09	4.2	10	115.9	0.6	4.1	1.0	200.5− 85.0	
11	124.565	0.006	0.10	2.7	10					128.3− 3.7	
12	126.845	0.003	0.08	26	10	127.0	0.5	28	6	144.6− 17.7	
13	132.55	0.03	0.12	0.25	···	···	···	···	···		
14	137.47	0.04	0.13	0.7	···	···	···	···	···		
15	140.906	0.003	0.06	38	10	141.2	0.5	41	8	144.6− 3.7	
16	153.15	0.06	0.15	1.1	25	153.8	0.7	1.1	0.3	790.4−637.2	
17	159.11	0.06	0.15	1.3	25	160.0	0.6	1.0	0.2	176.9− 17.7	b
18	159.33	0.06	0.15	0.9	25						b
19	176.863	0.003	0.09	88	10	177.1	0.6	97	20	176.9− 0	
20	182.785	0.005	0.09	32	10	182.9	0.6	38	9	200.5− 17.7	
21	185.96	0.03	0.15	0.35	···	186.5	0.8	6.0	1.5	823.2−637.2	
22	187.79	0.02	0.15	1	30					978.2−790.4	
23	200.520	0.014	0.3	3.2	10	200.7	0.5	3.4	0.7	200.5− 0	
23a	···	···	···	···	···	221.3	1.0	0.8	0.2		
24	231.21	0.07	0.3	0.8	30	231.5	0.6	1.3	0.4	978.2−747.0	
25	251.50	0.13	0.4	1.7	25	251.7	0.6	1.6	0.4	1041.9−790.4	
26	268.34	0.10	0.3	2.1	25	268.5	0.7	1.5	0.4		
26a	278.38	0.15	0.5	1.7	25	···	···	···	···		
27	294.81	0.17	0.6	2.9	25	294.8	0.6	2.7	0.6	1041.9−747.0	
27a	···	···	···	···	···	334.1	0.7	2.0	0.5		c
28	336.84	0.11	1.8	1.6	···	337.9	0.7	1.1	3.5		c,d
28a	341.58	0.03	0.9	7.3	15	···	···	···	···		e
29	352.75	0.12	0.9	2.1	25	353.0	0.7	1.8	0.5		
30	360.62	0.12	0.9	3.9	25	360.7	0.6	2.8	0.7	1150.9−790.4	
31	403.7	0.3	1.2	4.4	25	404.4	0.6	3.2	0.8	1150.9−747.0	
32	···	···	···	···	···	415.9	1.0	0.9	0.4	1119.8−703.6	
33	431.5	0.3	1.3	7.9	25	431.5	0.5	4.0	0.9		
34	···	···	···	···	···	439.8	0.7	3	1.0		
35	···	···	···	···	···	449.3	0.7	3.4	1.0		
36	460.0	0.4	1.5	11	25	460.1	0.5	9.5	2.0	637.2−176.9	
37	509.0	0.4	1.3	18	30	509.0	0.5	15	···	637.2−128.3	f
37a	516.6	0.6	2.0	13	25	···	···	···	···		e
38	527.83	0.19	1.3	10	···	528.7	0.6	4.3	1.5		
39	546.38	0.19	1.4	24	25	546.3	0.5	16	4	747.0−200.5	
40	557.4	0.3	1.5	16	···	557.8	0.6	14	4		
41	560.2	0.3	1.5	22	···	560.9	0.6	11	3		
42	569.9	0.4	1.5	16	···	569.9	0.6	10	3	747.0−176.9	
43	573.4	0.3	1.5	17	···	573.5	0.6	11	3	637.2− 63.7	
44	612.2	0.4	2.5	24	30	613.0	0.6	17	4		
45	619.9	0.7	2.5	24	···	620.2	0.6	20	5	637.2− 17.7	g
46	632.2	0.7	3	29	···	631.2	0.7	15	5	703.6− 72.3	g
47						634.2	0.7	13	4	637.2− 3.7	
48	645.7	0.13	3	47	20	646.3	0.5	34	7	790.4−144.6	
48a	654.9	0.4	3	7	···	···	···	···	···		d
49	665.6	0.8	3	8	···	663.6	0.8	2	0.6		d
50	686.1	0.8	3	6	···	687.2	0.8	9	2	703.6− 17.7	g
51	701.2	0.9	4	20	···	699.8	0.6	20	5	703.6− 3.7	g
52	···	···	···	···	···	705.5	0.8	7	2	790.4− 85.0	
53	718.8	0.9	4	10	25	718.6	0.6	5	1.5	790.4− 72.3	
54	729.9	0.9	4	11	25	729.5	0.6	9	2	747.0− 17.7	
55	···	···	···	···	···	738.0	0.7	6	1.5	823.2− 85.0	

In direct reaction theory, the cross section for a state is proportional to the spectroscopic factor. For the (d,p) reaction, this is the square of the overlap integral of the target ground state plus the incident neutron and the final state in the daughter nucleus. Thus for state $1J$ the spectroscopic factor will be pro-

TABLE VI (*Continued*).

1	2	3	4	5	6	7	8	9	10	11	12
	Crystal spectrometer					Ge(Li) diode					
Trans. No.	E_γ (keV)	ΔE_γ (keV)	FWHM (keV)	I_γ (rel)	100. $\Delta I_\gamma/I_\gamma$	E_γ (keV)	ΔE_γ (keV)	I_γ ($\gamma/10^3 n$)[a]	ΔI_γ ($\gamma/10^3 n$)	Assignments $E_i - E_f$	Comments
56	747.6	1.0	4	22	20	747.6	0.5	18	4	747.0 − 0	
57	...	...	...	...	...	753.1	1.5	2	1	823.2 − 72.3	
58	...	...	...	...	...	771.3	0.8	4	1.5	790.4 − 17.7	
59	790.5	1.2	4	15	30	790.5	0.6	6	2	790.4 − 0	
60	800.5	1.2	5	11	...	801.1	0.7	9	3	978.2 − 176.9	d
61	805.5	1.2	5	11	...	805.6	0.8	5	2	823.2 − 17.7	d
62						817.2	1.5	2.0	0.7		
63						823.4	0.8	4	1	823.2 − 0	
64						832.1	0.9	3	1		
65						844.3	1.0	3	1		
66						866.2	0.6	13	3	1041.9 − 176.9	
67						879.7	1.0	8	2		
68						894.1	0.6	10	3	978.2 − 85.0	
69						936.5	0.8	8	3		
70						943.7	0.9	8	2	1119.8 − 176.9	
71						957.5	0.7	14	3	1041.9 − 85.0	
72						966.7	2.5	4.0	1.6		
73						975.8	1.5	7	2	1150.9 − 176.9/ 1119.8 − 144.6/ 978.2 − 3.7	
74						991.2	0.6	16	4	1119.8 − 128.3	
75						1005.4	0.6	21	5	1150.9 − 144.6	
76						1024.7	0.8	3.0	1.2	1041.9 − 17.7	
77						1101.9	0.8	7	3	1119.8 − 17.7	
78						1107.9	0.7	13	4		
79						1131.1	1.2	6	2		
80						1138.1	1.2	7	2		
81						1150.7	0.6	23	5	1150.9 − 0	
82						1157.7	0.9	9	3		
83						1163.0	0.8	10	3		
84						1331.8	1.2	11	3		
85						1413.1	0.8	7	3		
86						1449.5	3.2	9	3		
87						1467.4	0.7	15	5		

[a] Based on $\sigma_c = (11.3 \pm 0.2)$ b for ^{141}Pr (BNL-325).
[b] The two transitions at 159 keV have been observed as an unresolved doublet in the diffraction-spectrometer experiment. They have been analyzed by a numerical least-squares fit.
[c] The separation of the 334- and 338-keV lines as a doublet with Ge(Li) diode is not unambiguous.
[d] Questionable line (diffraction spectrometer).
[e] Impurity line.
[f] This questionable line has been observed as a broadening of the annihilation line.
[g] Complex structure (diffraction-spectrometer experiment).

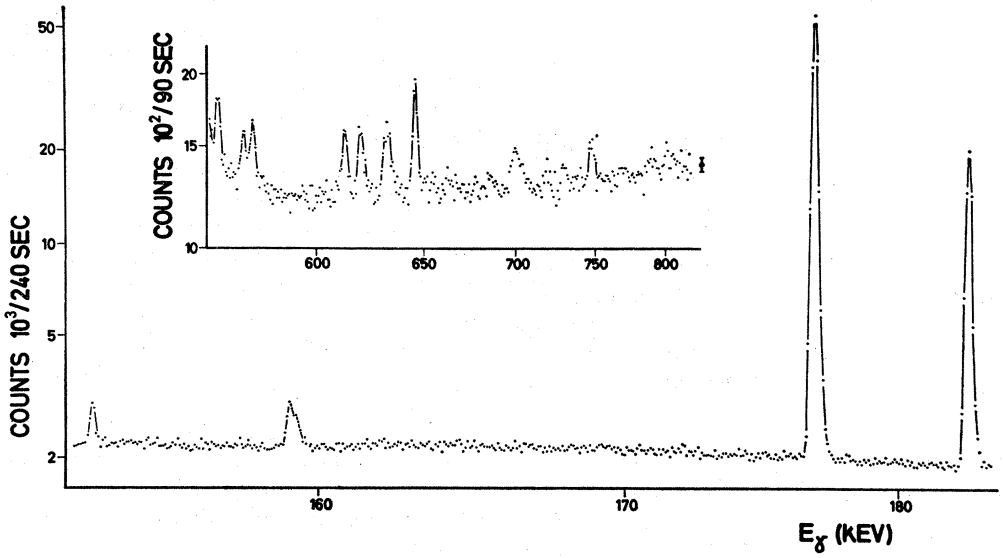

FIG. 5. Small section of the low-energy (n,γ) spectrum obtained with the diffraction spectrometer in second-order reflection between 159 and 183 keV and 560 and 806 keV.

TABLE VII. Normalized cross sections of the peaks g.s. to 7. Norm: Sum intensity g.s. to 7=100. Angular distribution: $l=3$ (see Fig. 2). The standard deviation is given beneath each value. For the average intensity, the error has been increased to 5% whenever the standard deviation was smaller in order to take into account nonstatistical errors.

Level	Energy (keV)	Normalized differential cross section 15°	25°	35°	45°	55°	65°	75°	105°	Average	Comments
g.s.	0.0 } 3.2 }	16	19	16	16	18	16	16	16	16.7	
	1.5	1	1	1	1	1	1	1	1	0.8	
1	17.8	3.2	5.7	4.5	7.1	3.8	5.7	5.6	4.4	5.0	
	0.6	0.5	0.6	0.7	0.7	0.4	0.6	0.4	0.8	0.5	
2	63.7	30	29	30	31	31	31	30	32	30.5	a
	0.2	2	2	2	2	2	2	2	2	1.5	
3	86.2	5.3	5.3	5.6	5.8	5.3	5.6	6.2	5.0	5.5	b
	0.7	0.6	0.5	0.5	0.7	0.4	0.5	0.4	0.5	0.3	
4	128.0	14	13	12	11	13	12	13	14	12.8	c
	0.4	1	1	1	1	1	1	1	1	0.6	
5	144.6	17	17	19	17	17	18	18	16	17.4	
	0.4	2	1	2	1	1	1	1	1	0.9	
6	176.8	10.4	9.6	10.4	9.3	9.7	9.9	9.4	10.5	9.9	d
	0.3	1.3	0.8	0.9	0.8	0.6	0.8	0.6	0.8	0.5	
7	200.8	3.5	2.7	2.9	2.0	1.9	2.0	1.6	1.3	2.3	e
	0.5	0.8	0.4	0.5	0.3	0.2	0.2	0.2	0.2	0.2	

[a] Impurity components (in μb/sr) subtracted: 5^{188}W at 15° (10).
[b] Impurity components (in μb/sr) subtracted: 3^{29}Si at 45° (25).
[c] Impurity components (in μb/sr) subtracted: 7^{32}P at 15° (5).
[d] Impurity components (in μb/sr) subtracted: 5^{33}S at 15° (10).
[e] Impurity components (in μb/sr) subtracted: 11^{36}Cl at 15° (15).

portional to $(2J+1)\alpha_{1J}^2$ while for state $2J$ it will be proportional to $(2J+1)\alpha_{2J}^2$. For $J=0$ and $J=7$ we have $\alpha_{1J}=\alpha_{2J}=0$; the two corresponding states are not expected to be populated in the (d,p) experiment. Since the relative phases of the states do not have importance for the interpretation of the (d,p) results, we choose them arbitrarily.

The group of peaks g.s. to 7 has an angular distribution corresponding to an l transfer of 3: the neutron is stripped into the $f_{7/2}$ orbital that we have been considering. Since the total experimental intensity has been normalized to 100 (see Table VII), we normalize the sum on the state-dependent parts of the spectroscopic factors for the levels of $1f_{7/2}$ parentage to the same value

$$2.08 \sum_{i=1,2} \sum_{J=1}^{6} \alpha_{iJ}^2(2J+1)=100,$$

where 2.08 is the normalization constant; the intensities in Table VIII are given by the expression

$$\text{intensity}=2.08(2J+1).$$

From a comparison of Tables VII and VIII we can draw two important conclusions: (1) The ground-state peak has a larger intensity than expected from its known spin 2, even if the state has the pure configuration $|\pi 2d_{5/2}\nu 2f_{7/2};2\rangle$. (2) The largest observed peak, peak 2, has a higher intensity than expected for a spin-6 state.

TABLE VIII. Expected sum intensity of a pair of levels with spin J.

J	1	2	3	4	5	6
Intensity	6.3	10.4	14.6	18.7	22.9	27.1

The only possible explanation for the large intensity of the ground-state peak is that it is a close doublet. When the energies of the levels disclosed through the high-energy (n,γ) data are matched to the pattern observed in the (d,p) experiment, it is seen that an excellent agreement (see Table IX) is obtained when the (d,p) energies are shifted upward by 1.6 keV. Under the assumption that the two components of the doublet are approximately equally intense, we can estimate its separation as twice the energy shift, namely 3.2 ± 1.5 keV. This is the value reported in Table II, where all energies are corrected for the difference between the true ground state and the peak centroid position.

The 71.9-keV level, seen in the high-energy (n,γ) data, has not been isolated in the (d,p) work. It lies close to the strongly populated level 2 at 63.7 keV; the intensity attributed to that state is in fact due to two levels. In this way the large (d,p) cross section of the level 2 can be explained.

The compound system formed through slow neutron capture has spin 2, spin 3, or both. Primary $E1$ or $M1$ transitions can populate low-lying levels with spins 1, 2, 3, or 2, 3, 4, or 1, 2, 3, 4 depending on the structure of the compound system. Therefore the levels with energies 17.7, 71.9, 144.7, 177.0, and 202.3 keV have spins J with $1\leq J\leq 4$.

It is also expected that $M1$ transitions within the configuration will be very much faster than any other competing multipole transition. Only $M1$ transitions should occur with measurable intensity, unless a level cannot undergo this mode of de-excitation.

A great deal of information about the spins of the

TABLE IX. Comparison of level energy values and configuration analysis.

Level nr.	Level energies (keV) (d,p)	High energy (n,γ)	Low energy (n,γ)	Spin	Relative (d,p) cross sections Experimental	Computed	State vectors α	$\lvert\beta\rvert$
g.s.	0.0	0.0	0.0	2	16.7±0.8	7.9	0.87	0.49
0	3.2±1.5		3.683±0.004	5		9.4	0.64	0.77
1	17.8±0.6	17.7±0.4	17.740±0.004	3	5.0±0.5	4.9	0.59	0.81
2	63.7±0.2		63.746±0.004	6	30.5±1.5	27.1	1.00	~0
2a		71.9±0.5	72.294±0.004	4		2.2	0.34	0.94
3	86.2±0.7		84.998±0.003	1	5.5±0.3	5.5	0.93	0.37
4	128.0±0.4		128.251±0.005	5	12.8±0.6	13.5	0.77	0.64
5	144.6±0.4	144.7±1.5	144.587±0.004	4	17.4±0.9	16.5	0.94	0.34
6	176.8±0.3	177.0±0.2	176.863±0.003	3	9.9±0.5	9.7	0.81	0.59
7	200.8±0.5	202.3±1.5	200.525±0.004	2	2.3±0.2	2.5	0.49	0.87

states can be gained from the spectroscopic factors extracted from the (d,p) intensities. In the following we describe the arguments on which we base our individual spin assignments. The analysis is summarized in Table IX and the decay scheme is shown in Fig. 6.

1. 176.9-keV Level

This level decays to the 2− ground state, restricting the spin to the values 1, 2, or 3. From the (d,p) intensities, it follows that spin 1 is impossible and spin 2 improbable. Therefore this level has probably spin 3.

2. 17.7-keV Level

A transition from the 176.9-keV level to this level suggests a spin 2, 3, or 4. Adding its (d,p) spectroscopic factor to that of the 176.9-keV level, we obtain 14.9, which is very close to the value expected for a pair of levels with spin 3, strongly suggesting this spin assignment.

3. 200.5-keV Level

The de-excitation of this state to the ground and to the 17.7-keV states requires that its spin is 2 or 3. The latter spin is ruled out on the basis of our model and the previous assignments; this gives spin 2 for this level. From the spectroscopic factor of this state we can deduce the magnitude of the components of the ground-state doublet.

4. 144.6-keV Level

The primary (n,γ) transition feeding this state requires a spin 1–4. Spins 2 and 3 are ruled out since the level pairs with these spins have already been assigned. The (d,p) cross section is too large for a spin 1. It must then have a spin 4.

5. 72.3-keV Level

Similar arguments and the intense 54.5-keV transition to the 17.7-keV state also imply spin 4 for this state.

6. 85-keV Level

This level is seen in the (d,p) spectrum and independently with help of the energy-combination principle applied to the accurately measured low-energy (n,γ) transitions. It is fed from the 2− state at 200.5 keV

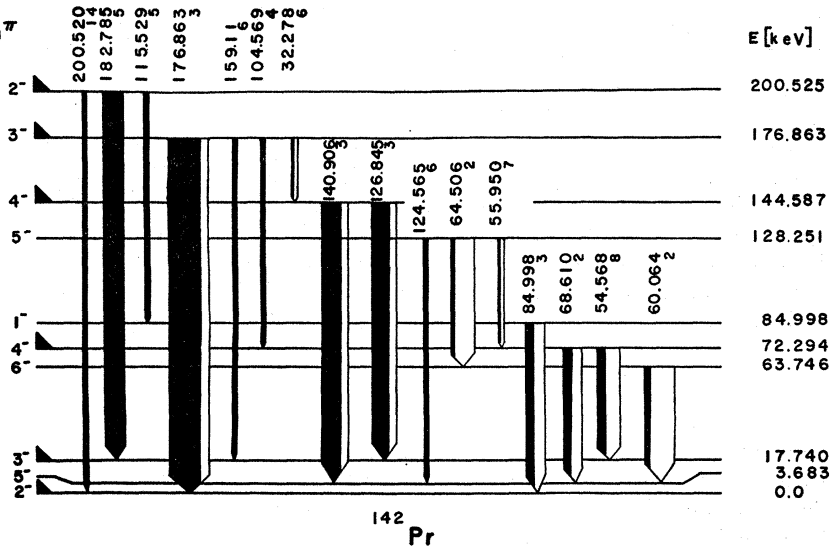

FIG. 6. Scheme of the low-lying nuclear levels in ^{142}Pr. The width of the black parts of the arrows indicates (nonlinearly) the γ-ray intensities. The white parts indicate in the same way the conversion electron intensities (calculated assuming pure $M1$ transitions). A full triangle directed upwards on the left end of a level shows that the state is populated by a direct (n,γ) transition. All states are populated in the (d,p) experiment; the 72.3-keV level could not be resolved from the strong 63.7 group, but there is indirect evidence that it has an appreciable (d,p) cross section.

TABLE X. Experimental and calculated branching ratios.

Initial state [keV]	J_i^π	Final state [keV]	J_f^π	E_i-E_f [keV]	E_γ [keV] Risø	LASL	I_γ Risø	LASL	Branching ratios Risø	LASL	R_{exp}	ΔR_{exp}	Calculated	Ratio No.
200.525	2⁻	0.0	2⁻	200.525	200.520	200.7	3.2	3.4	10	9	9.5	±1	9.6	1
					14	0.5	0.3	0.7						
		17.740	3⁻	182.785	182.785	182.9	32	38	100	100	100		100	
					5	0.6	4	9						
		84.998	1⁻	115.527	115.529	115.9	4.2	4.1	13	11	12	±1	12	2
					5	0.6	0.4	1.0						
176.863	3⁻	0.0	2⁻	176.863	176.863	177.1	88	97	100	100	100		100	
					3	0.6	9	20						
		17.740	3⁻	159.123	159.11	160.0	1.3	1.0	1.5	1[a]	1.3	±0.4	1.1	3
					6	0.6	0.4							
		72.294	4⁻	104.569	104.569	105.3	3.5	3.5	4.0	3.5	3.9	±0.4	3.9	4
					4	0.6	0.4	1.4						
		144.587	4⁻	32.276	32.278	32.5	2	5	2	5	2	±1	1.3	5
					6	2.5								
144.587	4⁻	3.683	5⁻	140.904	140.906	141.2	38	41	100	100	100		100	
					3	0.5	4	8						
		17.740	3⁻	126.847	126.845	127.0	26	28	70	63[a]	68	±10	70	6
					3	0.5	3	6						
		72.294	4⁻	72.293	...	...	...	...	...	...	...	...	0.01	
128.251	5⁻	3.683	5⁻	124.568	124.565	...	2.7	...	31	...	31	±3	31	7
					6		0.3							
		63.746	6⁻	64.505	64.506	64.7	8.8	8	100	100	100		100	
					2	0.5	0.9							
		72.294	4⁻	55.957	55.950	...	1.3	...	15	...	15	±4	14	8
					7									
72.294	4⁻	3.683	5⁻	68.611	68.610	68.7	8.1	9	100	100	100		100	
					2	5	0.8	5						
		17.740	3⁻	54.554	54.568	54.5	5.3	2	64	22[a]	20	±15	52	9
					8	6	1.0							

[a] The values denoted in the Los Alamos γ-ray intensity column should be decreased, as the Risø measurement shows that these transitions are complex.

and has therefore spin 1, an assignment also compatible with the (d,p) spectroscopic factor of this state.

7. 3.7-keV Level

This level is disclosed through the comparison of high-energy (n,γ) and (d,p) data. Its energy is found to be 3.683 keV through the application of the energy-combination principle, using the 140.9-, 126.8-, 68.6-, and 54.5-keV lines. The decay mode of the 72.3- and 144.6-keV levels and the (d,p) cross section (see Sec. III A 3) imply spin 5 for this state.

8. 128.3-keV Level

The 128.3 keV level has been observed in the (d,p) work and is confirmed by energy combinations. Its intensity in the (d,p) spectrum excludes a small spin; its spectroscopic factor, added to that of the 3.7-keV state is very close to the expected value for a pair of levels with spin 5, strongly suggesting this spin value. The assignment is confirmed by the γ decay of the level.

9. 63.7-keV Level

This state is obtained by the (d,p) data and a closed loop of low-energy γ lines. The large (d,p) spectroscopic factor implies a spin 6, an assignment supported by its decay to the 3.7-keV 5— state and by its population from the 128-keV 5— state.

Table IX shows that our spin assignments are in good agreement with the (d,p) spectroscopic factors for those cases where they have not been explicitly used. The amplitudes α and β of the wave function resulting from the analysis of these cross sections are listed in columns 8 and 9 of Table IX.

The level energies have been determined by a weighted least-squares fit of the transition energies. They are reported in Table IX for comparison with the (d,p) and high-energy (n,γ) values. The agreement between the level energy differences and observed transition energies can be seen from Table X.

An examination of Fig. 6 shows first that all transitions occur between states whose spin difference is equal to zero or one. This is in accordance with the expected $M1$ multipolarity of the transitions. Second, we see that nearly all transitions which are expected to be observable are in fact seen. The only missing transition is between the 144.6- and the 72.3-keV levels. We will discuss this point in Sec. III B, and find that the intensity of this transition is expected to be very weak.

We had expected the capturing state to have spin 2 and/or 3, but we note that the spins of the states populated by a direct γ transition from the compound state are 2, 3, and 4, suggesting that the capturing state has predominantly a spin 3. This cannot completely be ascertained, since the partial radiation widths

are governed by statistical laws,[28] and the weakness of the transitions leading to the 1− states may be accidental.

B. γ-Ray Branching Ratios

The study of γ-ray branching ratios provides an independent means of determining the state vectors. In Table X we present the experimental ratios that we have tried to fit. The theoretical values depend on three kinds of parameters: (a) the mixing parameters α and $|\beta|$, (b) the relative phases in the wave function, and (c) the values of the magnetic moments.

The details of the theoretical calculation are given in Ref. 27. Either Schmidt limits, effective moments deduced from measurements on odd-A neighboring isotopes, or arbitrary values can be chosen for the magnetic moment. In our first calculation we used the effective magnetic moments reported in Table XI, with the mixing amplitudes determined in the (d,p) experiment and varied the phases.

The interpretation of the (d,p) spectroscopic factors gives unambiguously the amplitude of the state vectors, but is insensitive to the phases. On the other hand, the branching ratios are sensitive to the amplitudes, to the phases, and to the gyromagnetic ratios, so that the result, with the number of ratios now available, is not unique. For this reason it is necessary to start the branching fit with the (d,p) amplitudes and try to adjust the phases so that these amplitudes give the better fit. Only then may the amplitudes be varied to get the final result. If the (d,p) amplitudes are not kept as a guide completely different state vectors may be obtained.

In order to compare the merits of the various fits, we defined the criterion for the goodness of fit as follows:

$$\chi^2=\frac{1}{N}\sum_{i=1}^{N}\left(\frac{R_{\mathrm{cal}}-R_{\mathrm{exp}}}{\Delta R_{\mathrm{exp}}}\right)_i^2.$$

R_{cal} represents the calculated branching ratio; R_{exp} and ΔR_{exp} are, respectively, the experimental ratio and its error (see Table X). N is the number (in this case nine) of ratios considered.

Using the (d,p) amplitudes and varying only the phases, the lowest value of χ^2 obtained was approximately 100. The phases are given in Table XII. In order to improve this value, we varied the amplitudes. Since the problem is not linear, it was solved by successive changes of the parameters in small steps. It was found that the α coefficient of the 144.6-keV level should be increased until the phases had to be reversed (see Table XIII). The best fit obtained then had a value of 4.0 for χ^2.

TABLE XI. Gyromagnetic ratios.

Shell	Schmidt limit	Effective moment	Adjusted moment
$g_{7/2}(p)$	0.49	0.794	0.794
$d_{5/2}(p)$	1.92	1.61	1.51
$f_{7/2}(n)$	−0.545	−0.28	−0.28

TABLE XII. Phases of the state vectors which fit best the branching ratios, using the (d,p) amplitudes.

Level [keV]	J^π	Phase	Level [keV]	J^π	Phase
0.0	2−	++	84.998	1−	+−
3.683	5−	+−	128.251	5−	++
17.740	3−	+−	144.587	4−	+−
63.746	6−	++	176.863	3−	++
72.294	4−	++	200.525	2−	+−

TABLE XIII. State vectors determined by the γ-ray branching fit.

Level energy [keV]	J^π	State vector α	State vector β	Level energy [keV]	J^π	State vector α	State vector β
0.0	2−	0.96	−0.28	84.998	1−	0.995	0.10
3.683	5−	0.63	−0.78	128.251	5−	0.78	0.63
17.740	3−	0.60	−0.80	144.587	4−	0.975	0.22
63.746	6−	0.997	0.07	176.863	3−	0.80	0.60
72.294	4−	0.22	−0.975	200.525	2−	0.28	0.96

At this point we studied the effect of the gyromagnetic ratios. The magnetic moment of the $g_{7/2}$ proton state has been measured in ^{139}La using nuclear resonance by Dickinson[29] and by Sheriff and Williams.[30] Their results are in excellent agreement and give $\mu=2.7781\pm0.0009$. The magnetic moment of the $d_{5/2}$ proton state in ^{141}Pr has been studied by many different methods.[31] In our analysis, we adopted 1.61 for the g factor of this state. The experimental uncertainty is about 10%. For the neutron in the $f_{7/2}$ shell, determinations of μ in ^{143}Nd and ^{141}Ce gave values between 0.9 and 1.3.[31] We took g equal to −0.28 as a starting value; these gyromagnetic ratios are given in Table XI. Varying the g factors of the $\pi g_{7/2}$ and $\nu f_{7/2}$ shell within reasonable limits did not change the fit significantly, so we kept the experimental values. However, decreasing the gyromagnetic factor for the $d_{5/2}$ shell appreciably improved the fit. Because the Schmidt value is appreciably larger than the effective value for this shell, the fit of the branching ratios with the Schmidt gyromagnetic ratios is very poor.

We could not at the beginning obtain a good fit for ratio No. 1 (see the last column of Table X) between the intensities of the 200.5- and 182.7-keV transitions. Since this ratio is mainly sensitive to the spin-2 wave function, we explored the whole possible range of ampli-

[28] H. E. Jackson, J. Julien, C. Samour, A. Bloch, C. Lopata, J. Morgenstern, H. Mann, and G. E. Thomas, Phys. Rev. Letters **17**, 656 (1966).

[29] W. C. Dickinson, Phys. Rev. **76**, 1414 (1959).

[30] R. E. Sheriff and D. Williams, Phys. Rev. **82**, 651 (1951).

[31] G. H. Fuller and V. M. Cohen, in *Nuclear Data Sheets*, compiled by K. Way *et al.* (U. S. Government Printing Office, National Academy of Sciences–National Research Council, Washington, D. C., 1965), Appendix 2.

tudes and phases of the 200.5-keV state. The value of this ratio as a function of the amplitude β of this 200.5-keV level is given in Fig. 7. We see that there is no solution within the estimated 10% error limits for the chosen phases (β of 200.5-keV level positive), but two for the reversed phases. The solution with the larger absolute value of β gives the better fit for the ratios No. 3, 4, and 5. It is also closer to the (d,p) results. Then the amplitudes for the other wave functions had to be readjusted and the phase of the spin-1 vector had to be also changed. We then obtained an excellent fit with χ^2 being 0.11. The calculated branching ratios are given in the next to last column of Table X.

The fit is excellent, but it is important to estimate properly the significance of this result. The parameters are six amplitudes (the phases can be taken into account in varying the amplitudes from -1 to $+1$) and, to a restricted extent, the magnetic moments. The number of free parameters is then almost the same as the number of values to be fitted (nine ratios). Since the problem is not linear, there exist several configurations which give acceptable fits to our experimental ratios. As an illustration, we present in Fig. 8 the variation of the γ-decay probability of the 200.5-keV state through the 115.5-keV transition as a function of the amplitude β of the 85-keV state (the 2— state vectors have the

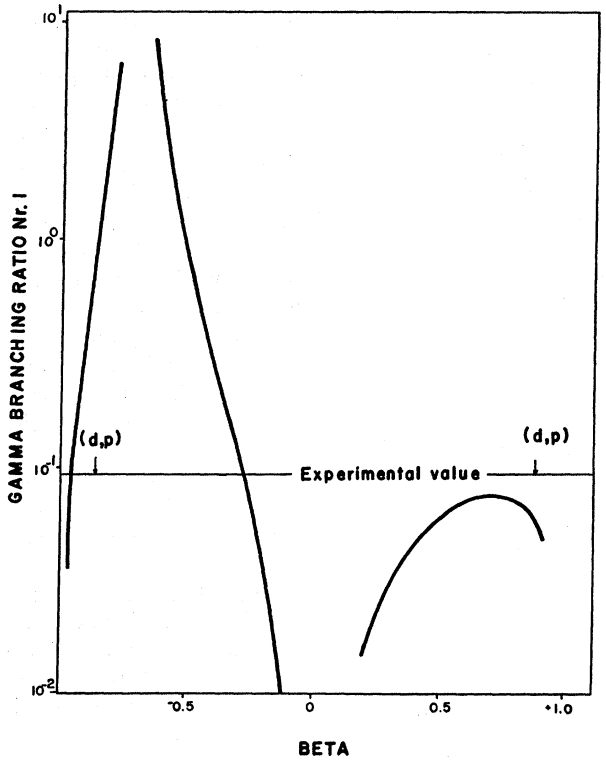

FIG. 7. Ratio of the 200.5 to the 182.8 keV γ-ray intensities as a function of the amplitude β of the 200.5-keV state vector. The spin-3 wave functions have the amplitudes and phases given in Table XIII.

values reported in Table XIII). We see that there are two different β amplitudes (-0.71 and 0.1) which give the probability of 8.8×10^9 sec^{-1} needed to fit the ratio No. 2 at the end of the procedure.

Slightly different configurations may also give approximately the same fit, since it is often possible to compensate the effect of the change of one parameter by other changes. We will not enter into a detailed discussion of the sensitivity of the results to each parameter, but state that, if the local solution is accepted, the accuracy of the determination of the parameters is, in general, within a few percent.

We stress that the given solution is the closest to the (d,p) results that we could find. This condition reflects our aim to find wave functions which satisfy all the experimental data. To find all possible solutions would not only require a large amount of computation but also would not be very meaningful.

Under these restrictions, we see that the state vectors of Table XIII are in excellent agreement with the vectors obtained in the analysis of the (d,p) amplitudes for the states with spin 3, 5, and 6. The agreement is acceptable for the 4— states but not for the spin-1 and -2 states. The spin-1 state vector enters only in one ratio and its discrepant value may be connected with the spin-2 amplitude disagreement. As shown in Fig. 8, we have two possible solutions for the spin-1 state; both of them are about equally in disagreement with the (d,p) results. We have given in Table XIII the vector which was perhaps the closest.

The differences between the state vectors obtained by the two methods are probably due to the fact that the γ-ray transition probabilities are much more sensitive to the impurities in the wave function and to the truncation of the vector basis system than the (d,p) amplitudes are.

From the results we note that the transition between the levels at 144.5 and 72.3 keV has a very small probability. Its expected intensity is below our present experimental capability. A 24-keV transition between the 200.5- and the 176.9-keV levels is also expected to be very weak.

C. 15-min Isomeric State

According to our level scheme (see Sec. III A), there should be a spin-5 level at 3.683 keV with a measurable half-life. In a special experiment[32] the activity of the 1.57-MeV transition in ^{142}Nd (see Fig. 9) was observed as a function of time. From the analysis of the data a half-life of 14.6 ± 0.5 min was obtained for the isomeric state, and the cross-section ratio for the formation of the 5— isomeric state to that of the 2— ground state in ^{142}Pr was found to be 0.52 ± 0.04.

If we adopt the value 11.3 ± 0.2 b (cf. Sec. II B) for

[32] J. Kern, G. Mauron, and B. Michaud, Phys. Letters **24B**, 400 (1967).

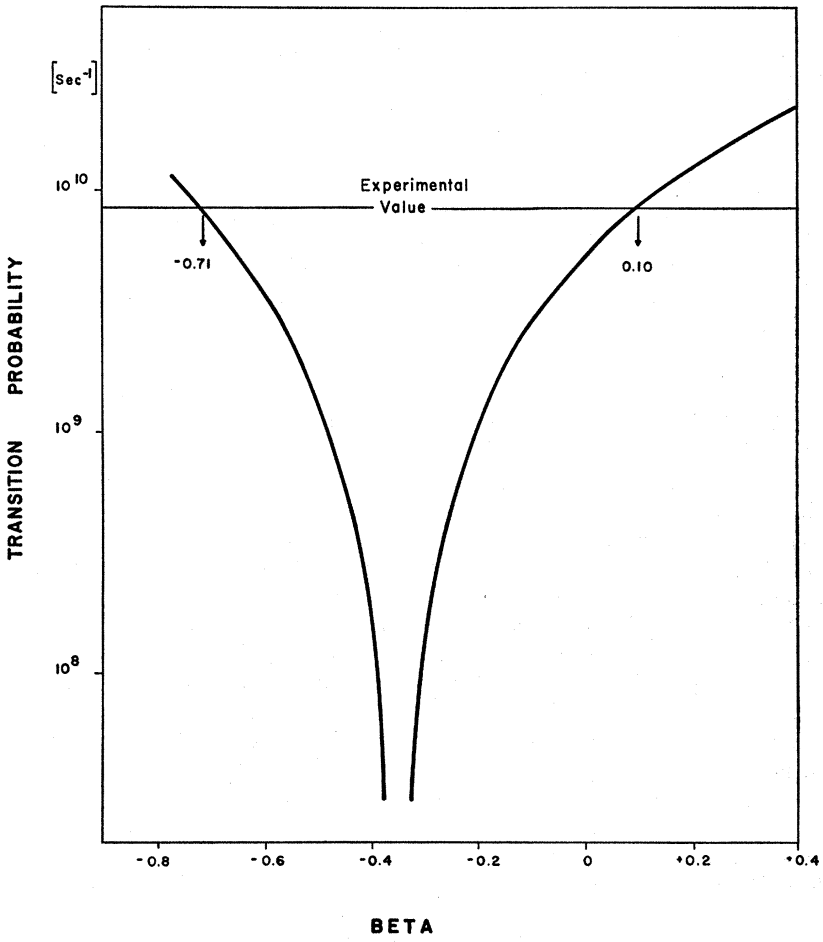

FIG. 8. Variation of the γ-decay probability of the 200.5-keV level through the 115.5-keV transition as a function of the β amplitude of the 85-keV state. The transition probability of 8.8×10^{9} sec^{-1} is needed to fit the ratio No. 2 at the end of the procedure when the 2− state vectors have the amplitudes and phases given in Table XIII.

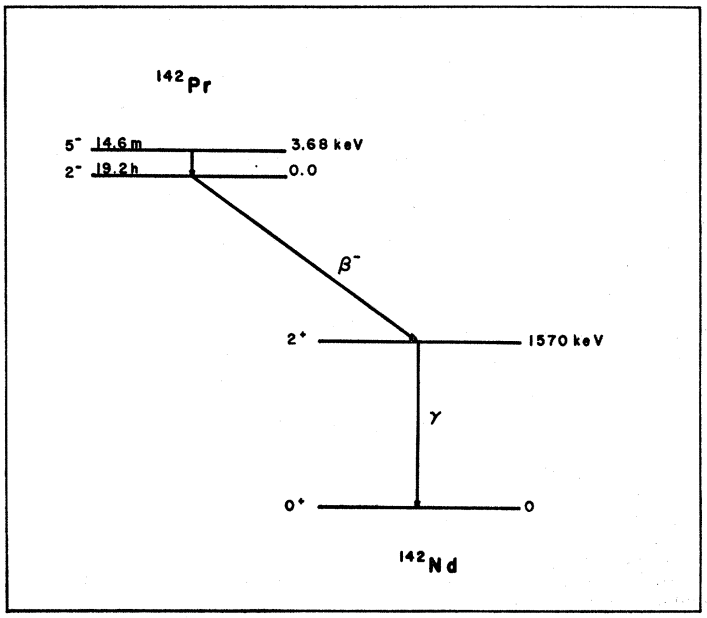

FIG. 9. Decay scheme of the 5− isomeric state.

TABLE XIV. M-subshell conversion coefficients for $M3$ and $E4$ multipolarities and for 3.683 keV in $_{59}$Pr. The calculated electron binding energies ϵ_{cal} are given in the second column. Source: H. C. Pauli (private communication).

Subshell	ϵ_{cal} [keV]	$\left(\frac{\epsilon_{exp}-\epsilon_{cal}}{\epsilon_{cal}}\right)$ %	$\beta^{(0)}(M3)$	$\alpha^{(0)}(E4)$
M_{I}	1.510	−0.138	0.620(9)	...
M_{II}	1.359	−1.60	0.736(7)	0.245(12)
M_{III}	1.259	−1.70	0.935(10)	0.344(12)
M_{IV}	0.987	−3.67	0.651(8)	0.221(13)
M_{V}	0.965	−3.40	0.249(9)	0.310(13)
M_{total}			1.03(10)	0.59 (13)

the total activation neutron-capture cross section, the activation cross section of the isomer is 3.9±0.4 b.

To obtain the experimental γ-ray transition probability, it is necessary to know the conversion coefficient. The small energy of the transition allows conversion only in the M and higher shells. Using results obtained without screening[33,34] and empirical corrections,[35] the $M3$ total conversion coefficient was first estimated to be 3×10^{9} and the half-life as about 7 min.[32] Since this estimate was crude, a theoretical calculation was undertaken by Pauli of the University of Basle. Although the low energy of the emerging electron makes it difficult to normalize the outgoing wave function, Pauli's calculation did converge. The calculated values are reported in Table XIV. The finite size of the nucleus has been taken into account as it was in the calculation by Rose.[33] Dynamical effects are expected to be small and could be included easily.[36] Screening is also included; the screening function was obtained by a nonrelativistic Hartree-Fock calculation. The binding energies were very satisfactorily reproduced with an accuracy better than 4%. The error on the conversion coefficient is expected to be less than 5%. For comparison, a calculation with the Thomas-Fermi-Dirac function gave less precise results,[36] which do not differ by more than 10%.

If conversion in the N and higher shells is neglected, the experimental γ-transition probability is $\lambda_\gamma=7.7\times10^{-14}$ sec^{-1}. To our knowledge, calculations of conversion coefficients in the N and higher shells have not been performed. Such calculations are more difficult than for the M shell. Experimental values for other multipolarities and energies indicate that the M/N conversion ratio is of the order of 3. If this is also true here, we obtain the value $\lambda_\gamma=(5.8\pm1.0)\times10^{-14}$ sec^{-1}.

As a further test of the wave functions we have computed this transition probability. Since the spin-5 wave function determined in the (d,p) experiment and the branching fit are in good agreement, we have studied the transition probability only as a function of the ground-state wave function. The result is reproduced graphically in Fig. 10. The following two possible state vectors $|\alpha;\beta\rangle$ give the experimental transition probability:

$$|0.69\pm0.04;\ 0.72\pm0.04\rangle$$

or

$$|0.48\pm0.05;\ -0.88\pm0.03\rangle.$$

The agreement with either the value given in Table IX or Table XIII is poor. An agreement could be obtained with a conversion coefficient intermediate between the calculated value and the estimate of Kern *et al.*[32] However, agreement within a factor of 2 for such an absolute transition probability can be considered satisfactory, especially when it is considered that core-polarization effects have been neglected in the calculation.

The interpretation of the (n,γ) results allows us to make estimates of the relative population of the isomeric and ground state. We have summed the intensities of all transitions represented in Fig. 6 leading to the 3.68-keV isomeric level and to the levels of 0 and 17.7 keV, assuming theoretical $M1$ conversion coefficients. To the second sum we must add the intensities of the 5843- and 5826-keV transitions feeding the ground state and 17.7-keV states directly from the capturing state. We find that the first sum is 54% of the second, which is in excellent agreement with the observed value of 52±4%. The intensities considered account for

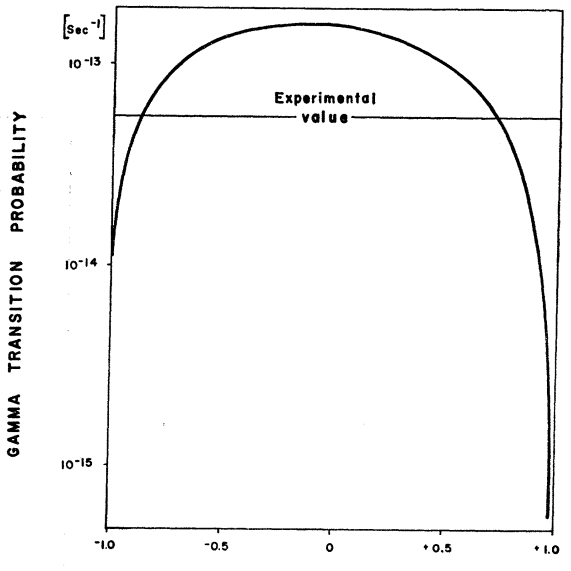

FIG. 10. Decay probability of the 3.68-keV isomeric level to the ground state through an $M3$ γ transition as an function of the β amplitude of the ground-state vector. The 5— state vector amplitudes have the values reported in Table XIII.

[33] M. E. Rose, *Internal Conversion Coefficients* (North-Holland Publishing Co., Amsterdam, 1958).
[34] R. F. Connell and C. O. Caroll, Phys. Rev. **138**, B1042 (1965).
[35] Y. Y. Chu and M. L. Perlman, Phys. Rev. **135**, B319 (1964).
[36] H. C. Pauli, Helv. Phys. Acta **40**, 713 (1967); and (private communication).

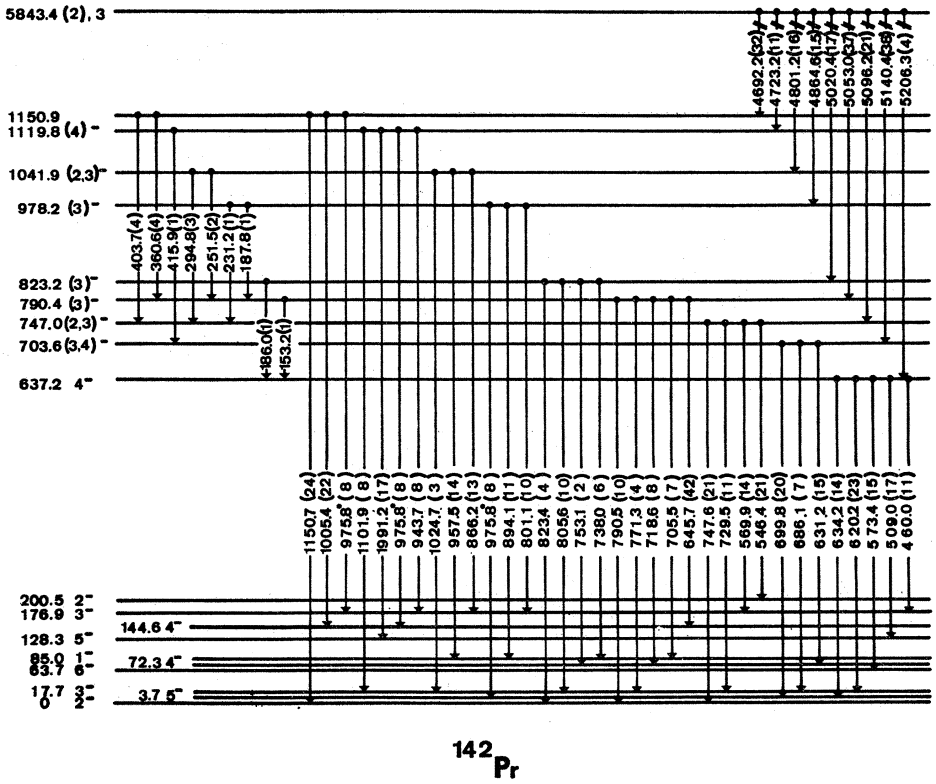

FIG. 11. Tentative γ-decay of the levels between 600- and 1150-keV excitation. The transitions denoted by an asterisk can be located at several places in the scheme. The energy of the more precise determination is noted. The average intensity is given between parentheses.

something over one half of the capture events. The remaining intensity involves transitions coming from intermediate energy levels. Some of these have been tentatively assigned in Fig. 11. The levels in this part of the scheme mostly have small spins and decay predominantly to the ground state. When these transitions are taken into account, the ratio reduces to 48%.

The isomeric cross-section ratio can also be compared with theoretical predictions.[37,38] Since the spins of the levels under discussion ($I=2$ and 5) are not very far from the spin of the compound state ($I=3$), the result will not depend very strongly on the γ-ray multiplicity N_γ, but rather on the parameter σ which characterizes the spin dependence of the nuclear level density. Using the simple numerical results of Huizenga and Vandenbosch,[37] with $N_\gamma=3$ and $\sigma=3$, we have obtained the ratio $0.3/0.7=0.43$ and for $\sigma=5$ the ratio 0.79, which bracket our experimental value (0.52 ± 0.04).

D. Higher Excited States

1. Level Scheme Between 600 and 1160 keV

Almost all the levels observed in the (d,p) reaction in this energy range have also been populated in the high-energy (n,γ) experiment. The exceptions are the levels around 1120 keV. The levels 1115.4 and 1127.2 keV result from analyzing a proton group as a doublet. This line is clearly too wide to be single level around 1120 keV as observed in the (n,γ) experiment; the experimental information is not sufficient to determine whether it has more than two components. It is possible that the components may have different l dependences, since the angular distribution of the group could not be interpreted.

Since the population of many levels by primary transitions in the (n,γ) reaction is relatively large, their decay should be observable. It was possible to assign a large fraction (see Table VI) of the low-energy capture γ rays as transitions from these levels (Fig. 11). When a transition was observed both with the Ge diode and with the curved-crystal spectrometer, we give the energy of the more precise determination; the average intensity is shown in parentheses. Only a few transitions (denoted by asterisks) have multiple locations. Precise level energies result from a least-squares fit of the transition energies. They are compared with the (d,p) and the high-energy (n,γ) results in Table XV. In applying the energy-combination principle, it is possible to construct many levels, but we rejected those which were not in agreement with the high-energy (n,γ) results. In some cases, levels with slightly different energies but different decay modes can be considered, for instance at 704.4 ±0.1 keV. Regarding the (d,p) data, we note some very good agreements (levels at 637 and 823 keV), some acceptable differences (levels at 748 and 793 keV), and

[37] J. R. Huizenga and R. Vanderbosch, Phys. Rev. **120**, 1305 (1960).
[38] D. Sperber, Nucl. Phys. **A90**, 665 (1967).

TABLE XV. Comparison of the energies and summary of the properties of the higher-energy levels. The relative (d,p) cross sections are taken from Table XVII.

Level No.	(d,p) Energy [keV]	(d,p) l transfer	(d,p) Relative cross section	High-energy (n,γ) Energy [keV]	Low-energy (n,γ) Energy [keV]	J^π
8	637.2±0.5	1	45.8	637.1±0.3	637.2±0.1	4−
9	705.8±0.4	1	6.4	703.0±0.3	703.6±0.3	(3−, 4−)
10	748.2±0.6	1	22.9	747.2±0.3	747.0±0.1	(2−, 3−)
11	792.1±0.6	1	24.6	790.4±0.4	790.4±0.1	(3−)
12	823.5±0.7	1	3.4	823.0±0.6	823.2±0.1	(3−)
13	981.3±0.7	1	11.7	978.8±1.5	978.2±0.1	(3−)
14	1045.2±0.7	1	17.9	1042.6±0.3	1041.9±0.1	(2−, 3−)
15	1115.4±1.2	...		...	...	
15a	...			1120.2±0.3	1119.8±0.3	(4−)
16	1127.2±1.8	...		...	...	
17	1154.4±0.9	1	6.2	1151.2±0.3	1150.9±0.1	

some very large differences (levels at 706, 981, 1045, and 1154 keV), the (d,p) energy being systematically larger. It is probable that some levels have an undisclosed complex structure, but we must also consider a slight miscalibration of 1 to 2 keV in this region.

TABLE XVI. Comparison of the energies and summary of the properties of the higher-energy levels.

Level No.	(d,p) Energy [keV]	(d,p) l transfer	High-energy (n,γ) Energy [keV]
18	1183.3		
19	1200.4		
20	1220.2		
21	1255.2	(1)	1251.8
22	1269.6	(1)	1264.2
23	1348.2		1348.6
24	1362.7		
25	1381.5		
26	1395.2		1396.4
27	1408.2		1405.2
28	1428.9		
29	1462.7	(1)	
30	1473.5	(1)	1473.6
31	1499.1	1	1500.1
32	1519.8	1	
33	1540.1	1	
34	1556.0		
35	1570.7	(3)	1569.4
36	1586.7	(3)	
37	1597.4	(3)	1594.3
38	1621.6		
39	1642.6	(1)	
40	1660.1	1	
40a	...		1670.1
41	1677.2	1	
41a	...		1683.0
42	1693.5	1	
43	1711.2		1713.0
44	1725.8		1730.0
45	1755.2	1	1754.9
46	1771.5	1	
47	1799.5	1	1794.3
48	1812.2	1	
49	1832.3	1	1833.7
50	1845.1	1	1845.6
51	1866.2	(1)	
52	1884.6	(1)	
53	1900.8	(1)	1901.9
54	1919.4	1	1922.9
55	1934.9	1	1935.7
56	1957.4	1	1954.3
57	1982.9		1984.0
58	2001.2		
59	2015.5		

2. *Levels above 1160 keV*

Since the level density becomes large at the higher excitation energies, it is not always certain that a given level is correctly identified as being excited by both the (d,p) and (n,γ) reactions. A comparison of the results is given in Table XVI. Above 1300 keV, the (d,p) and (n,γ) results match fairly well for a number of levels. The l transfer obtained by the proton angular distributions (see Fig. 2) is given in a separate column. Our l assignments do not always agree with those of Fulmer *et al.*[1] They found that the angular distributions of the levels between 1.42 and 1.97 MeV probably correspond to a transfer of $l=3$. In the same region we find only a few levels with a possible $l=3$ angular distribution, and numerous levels observed above 1640 keV exhibit $l=1$ angular distributions very clearly. The small number of levels with an $l=3$ distribution is puzzling. It is known from studies in the odd-A nuclei with 83 neutrons[2,39,40] that a level with appreciable cross section at 1560 keV in ^{143}Nd and 1500 keV in ^{141}Ce has the $l=3$ distribution. In view of the many good $l=1$ distributions, we can exclude a systematic experimental error. Our only explanation is that we have almost no group of protons with a single l component in this region. Since the cross section for $l=1$ stripping is generally appreciably larger than for $l=3$, the latter distributions may no longer be recognizable.

3. *Discussion of the Results*

The interpretation of our results demands first an understanding of the levels of the neighboring odd-A nuclei. In spite of recent developments, a satisfactory coupling scheme is still lacking. It had been proposed[1] that the two low-lying $l=1$ levels in ^{141}Ce (at 660 and 1009 keV) and in ^{143}Nd (at 740 and 1305 keV) are due to

[39] C. L. Nealy and R. K. Sheline, Phys. Rev. **155**, 1314 (1967).
[40] P. R. Christensen, B. Herskind, R. R. Borchers, and L. Westgaard, Nucl. Phys. **A102**, 481 (1967).

TABLE XVII. Relative cross sections of peaks 8, 9, 10, 11, 12, 13, 14, and 17. The values have been normalized to a value of 100 for the combined cross section of peaks 8, 9, 10, and 11. Angular distribution: $l=1$ (see Fig. 2). The standard deviation is given beneath each value.

Level	Energy (keV)	Normalized differential cross section 15°	25°	35°	45°	55°	65°	75°	90°	105°	Average	Comments
8	637.2	48	46	43	44	46	48	48	43	47	45.8	
	0.5	3	3	3	3	3	3	3	3	3	0.6	
9	705.8	5.8	6.4	6.9	6.8	6.7	6.7	6.0		5.8	6.4	
	0.4	0.7	0.5	0.7	0.8	0.5	0.5	1.1		0.5	0.2	
10	748.2	23	23	24	24	24	21	22		23	22.9	
	0.6	1	2	2	2	1	1	1		1	0.4	
11	792.1	24	24	26	25	24	25	24		25	24.6	a
	0.6	2	2	2	2	1	2	1		2	0.2	
12	823.5	4.2	3.4	2.2	4.7	2.6	3.1	3.5		3.5	3.4	
	0.7	0.6	0.3	0.4	0.5	0.3	0.3	0.3		0.7	0.3	
13	981.3	13	11	13	11	12	12	11	12	12	11.7	
	0.7	1	1	1	1	1	1	1	1	1	0.2	
14	1045.2		18	20	18	18	16	17	19	18	17.9	
	0.7		1	1	1	1	1	1	1	1	0.4	
17	1154.4	7.9		6.4	6.4	6.1	6.4	6.1		5.6	6.2	b,c
	0.9	2.6		1.2	0.5	0.5	0.7	0.5		0.5	0.2	

[a] An impurity component (10 μb/sr) due to ^{24}Na has been subtracted at 15°.
[b] Average value is a weighted average.
[c] A background due to the tail of a ^{13}C peak has been subtracted at 15°.

the splitting of the $p_{3/2}$ particle state. This state would be mixed with the $\frac{3}{2}-$ state which is formed by a coupling of the $f_{7/2}$ neutron with the 2+ first excited state of the neighboring even nuclei.[1] This interpretation is no longer possible since the upper level has been found to have a spin of $\frac{1}{2}$.[40,41] The question of the coupling is then still not solved.

The summed cross section of levels g.s. to 7 in the (d,p) experiment is found to be 1429 μb/sr at 45°, which is in excellent agreement with the cross section (1433 μb/sr) of the ground state in ^{143}Nd.[39,42] The next level in ^{143}Nd has a cross section of 1769 μb/sr. To obtain a similar cross section in ^{142}Pr, it is necessary to sum the cross section of all levels from 637 keV to 1154 keV (see Sec. III D 1). With the exception of the levels No. 15 and 16 which have no clear angular distribution, the relative intensities of all these groups are given in Table XVII.

The coupling of a $J=\frac{3}{2}-$ level with $d_{5/2}$ and $g_{7/2}$ quasiprotons should result in the following levels:

$$\pi d_{5/2}: \quad 1-, 2-, 3-, 4-,$$
$$\pi g_{7/2}: \quad 2-, 3-, 4-, 5-.$$

Following arguments similar to those given in Sec. III A, i.e., assuming mixing of the states with the same spin and parity, seven states should be observed with spins 1 to 4. Since we observe more states, this simple picture is not correct and mixing with other configurations must be considered.

From Table XVII we see that the level at 637 keV has twice the intensity of any other level. This suggests that the level has a relatively large spin. On the other hand, since it is directly populated by a high-energy (n,γ) transition, the highest possible value could be 4. We consider this the probable value.

The l-value difference between the group of levels from 600 to 1150 keV and the group near the ground state is 2. The multipolarity of the radiations between levels of the two groups is then expected to be $E2$. Within the upper group, $M1$ transitions may be dominant as they are in the lower group. We have made this assumption in trying to determine the spins of some levels. Application of a $(2I+1)$ rule for the spectroscopic factor, and taking into account mixing, was not successful. Our conclusions, which are tentative, are presented in Fig. 11.

IV. SUMMARY

Prior to our investigation of ^{142}Pr by (d,p) and (n,γ) reactions, the details of the low-energy structure were nearly completely unknown. The present combination of (d,p) and (n,γ) experiments has revealed considerably more detail about the low-lying levels in ^{142}Pr, mainly because of the better resolution and precision of the data.

To interpret all the results, we adopted a simple nuclear model for ^{142}Pr in which a quasiproton and a neutron are assumed to interact through a neutron-proton two-body residual interaction. We consider that the levels exist in two distinct regions. The first region contains the levels below 250 keV and we assume that only the configurations

$$|\pi 2d^0_{5/2}\nu 2f_{7/2}J;00;JM\rangle$$
and $$|\pi 1g^0_{7/2}\nu 2f_{7/2}J;00;JM\rangle$$

are important. There should then be 14 low-energy

[41] L. Veeser, J. Ellis, and W. Haeberli, Phys. Rev. Letters **18**, 1063 (1967).
[42] It must be noted that the (d,p) experiment in ^{142}Pr was performed at the same time and using the same technique as the experiment on ^{143}Nd performed by Nealy and Sheline (Ref. 39). Thus some systematic errors may be the same in both cases.

levels. Without configuration mixing, only the six levels from the

$$|\pi 2d^0_{5/2}\nu 2f_{7/2}J;00;JM\rangle$$

configuration would be observed in the (d,p) reaction. However, since the neutron-proton residual interaction can mix states of the same spin and parity arising from these two configurations, we might expect to see all the states except the two with spin 0 and 7. From our results, it has been possible to deduce the spins. The (d,p) intensities give the mixing amplitudes in the wave function in a straightforward manner. In addition to not seeing the states of spin 0 and 7, we see only one of the states with spins 1 and 6. From the (d,p) intensities, we conclude that the spin-6 states are not mixed and so the $|2g^0_{7/2}2f_{7/2}6;00;66\rangle$ state should not be observed directly in any of the experiments performed here. Although the spin-1 states are mixed, weighting of the cross section by the $(2J+1)$ rule would make it difficult to observe the second spin-1 state in the (d,p) experiment. Also, since spin 3 predominates as the capturing state, the spin-1 states are not populated directly in the high-energy (n,γ) experiment. Since the spin assignments from the (d,p) data were ambiguous, the (n,γ) data was crucial in making several assignments. The low-energy γ rays fit into the level scheme in a very consistent manner. As a further test for determining the wave functions, we assumed the same model space that was used in the analysis of the (d,p) data and performed a least-squares fit to the branching ratios, varying the wave-function amplitudes and phases. The wave functions obtained from the (d,p) data and the (n,γ) results are in satisfactory agreement, especially when the drastic truncation used in the calculation is considered.

The 3.7-keV state was found to have spin 5. Since it can only decay to the ground state by an $M3$ transition, we expect a long-lived isomeric state. This isomer was disclosed in a separate experiment[32] and found to have a half-life of 14.6 min. We computed the theoretical transition probability, which was found to be within a factor of 2 of the experimental value. Since we have neglected core-polarization effects, this agreement seems quite satisfactory.

Above 250 keV, it has been possible only to make speculative interpretations. The decay pattern of a group of levels between 600 and 1160 keV has been deduced with few ambiguities. By making the assumption that transitions in this set of levels are $M1$ and those between this set and the set below 250 keV are $E2$, it has been possible to tentatively assign some spin values. However, a simple model interpretation similar to the one described for (d,p) results below 250 keV fails. This should not be surprising, since we are now considering the region of several quasiparticle excitations and various collective states.

Many more detailed experiments will be necessary in order to elucidate the structure of the levels above 250 keV and to detect further admixtures in the lower levels. We hope that the growing body of detailed experimental information will stimulate theorists to study the unexplored problem of heavy odd-odd nuclei.

ACKNOWLEDGMENTS

We are very grateful to Professor O. Huber, Professor H. Maier-Leibnitz, Professor O. Kofoed Hansen, Professor T. Bjerge, and Dr. H. T. Motz for their continuous interest in and sponsorship of this work. We express our thanks to Dr. H. C. Pauli (Basle) for performing the calculation of the 3.7-keV $M3$ conversion coefficient, and to Dr. T. Udagawa for several fruitful discussions. We sincerely thank the staffs of the reactors and of the computing centers of our laboratories. One of us (J. K.) is thankful for permission to use the IBM 7040 of the EPUL in Lausanne and the CDC 6600 of CERN in Geneva. The assistance of Dr. C. Nealy and of the crew of the FSU Tandem Van de Graaff in taking the (d,p) data and the careful plate-counting of Mrs. M. Jones, Mrs. S. Hipps, and Mrs. E.-J. Wehunt are gratefully acknowledged.